dihydroxyvitamin D) were measured at the beginning of the study [14,15]. Serum midportion-parathyroid hormone (PTH) was measured by using a double-antibody immunoradiometric method [16] and osteocalcin by an immunoradiometric assay at the beginning of the study and every 12 weeks thereafter, along with routine blood count, biochemical tests including serum Ca, P, and alkaline phosphatase, and urinalysis.

Statistical analysis was conducted by Student's *t* test, Tukey test, and Wilcoxson signed rank test. Lumbar BMD data were subjected to intention-to-treat (ITT) analysis without exclusion cases, filling defective sites with change-free values. The occurrence of new fractures was analyzed by odds ratio estimates in a logistic procedure.

Results

Of the 414 test subjects who entered the study, data on 406 subjects, 135 from Group A, 133 from Group B, and 138 from Group C were analyzed after exclusion of 8 subjects: 1 for not conforming to the admission criteria of the study because of an associated disease, 2 for being subjected to other forms of therapy for osteoporosis interfering with the evaluation of the results, 4 for failing to show up after the initial visit and 1 for failing to withhold the treatment during the 8 weeks of the washout period. Administration of the test drug had to be discontinued before the 36th week, precluding the planned final measurement at the 48th week in 26, 23, and 26 subjects in groups A, B, and C, respectively. The reasons for the discontinuation and dropout are summarized in Table 2. DXA measurement proved to be unacceptable because of scoliosis, spondylosis deformans, ligamentous calcification, or localized hyperosteosis in 23, 26, and 23 subjects in Groups A, B, and C, respectively. In total, 49 subjects were excluded from each group, making the total number of subjects with analyzable DXA data 83 in Group A, 85 in Group B, and 88 in Group C, a total of 256 subjects. After exclusion of subjects in whom differentiation of the osteoporotic and nonosteoporotic causes of pain was difficult, data from 340 subjects were analyzed for pain assessment.

The prestudy background of the test subjects in these three groups are shown in Tables 3, 4, and 5. Each group consisted mainly of females with a small number of males. Mean age, time after menopause, body weight, number of spinal fractures, and spinal BMD were indistinguishable among the three groups, confirming the homogeneity of the patients. No evidence of vitamin D deficiency or marked secondary hyperparathyroidism was found in any of these patients. The criteria for the diagnosis of osteoporosis adopted in the present study were intended to exclude nonosteoporotic decrease of BMD such as osteomalacia and primary hyperparathyroidism. Compared to the current criteria by the World Health Organization (WHO) or the Japanese Society of Bone and Mineral Research, it may tend to overemphasize the frequency of confounding nonosteoporotic conditions. In view of the mean lumbar BMD of 0.714 ± 0.124 (mean ± SD), median of 0.712, and 25%–75% range of 0.621–0.801 g/cm^2 in Group A, 0.717 ± 0.131, 0.703, and 0.626–0.790, respectively, in Group B, and 0.716 ± 0.133, 0.731, and 0.608–0.803, respectively, in Group C as the QDR-1000 equivalent, most of the subjects appear to conform the current criteria for osteoporosis, i.e., less than −2.5 SD (WHO) or −30% from the young adult mean (0.708 g/cm^2). BMD values were converted to QDR-100 equivalent by calculation using the equations shown in Sone et al. [17].

As shown in Fig. 1, spinal BMD significantly increased from the baseline level after 12 weeks in Group A and after 24 weeks in Group B, and was maintained at approximately the same level in Group C. The mean percent change of spinal BMD at the end of the trial was +3.4% in Group A, +2.4% in Group B, and −0.5% in Group C. The values for Groups A and B were both significantly higher that for

Table 2. Summary of the reasons for discontinuation or dropout

Reasons	A	B	C	Total
Discontinuation				
Complications or their aggravation	1 (1)	2 (2)	2 (1)	5 (1)
Drug-related adverse events	4 (3)	1 (1)	2 (1)	7 (2)
Refusal by patient	3 (2)	0 (0)	0 (0)	3 (1)
Irregular timing for consultation	0 (0)	1 (1)	0 (0)	1 (0)
Irregular timing for drug ingestion	1 (1)	0 (0)	0 (0)	1 (0)
Others	0 (0)	4 (3)	2 (1)	6 (1)
Dropout				
Improvement of subjective symptoms	4 (3)	7 (5)	3 (2)	14 (3)
Absence of effect	1 (1)	0 (0)	0 (0)	1 (0)
Complication and their aggravation	0 (0)	1 (1)	1 (1)	2 (0)
Drug-related adverse events	0 (0)	0 (0)	1 (1)	1 (0)
Burdens of housework or business	3 (2)	3 (2)	3 (2)	9 (2)
Poor cooperation by patients	4 (3)	7 (5)	9 (7)	20 (5)
Change of physician or clinic	1 (1)	2 (2)	0 (0)	3 (1)
Others	1 (1)	3 (2)	4 (3)	8 (2)
Totals	23 (17)	31 (23)	27 (20)	81 (20)

Numbers of subjects are followed by numbers in parentheses indicating percentage of the total number of the subjects in the group

Table 3. General prestudy background data in 406 subjects

Group	A	B	C	Total	Results of statistical analysis
Total number of patients	135	133	138	406	
Sex					
Males	10 (7)	7 (5)	6 (4)	23 (6)	NS
Females	125 (93)	126 (95)	132 (96)	383 (94)	
Age (years)					
-59	30 (22)	28 (21)	26 (19)	84 (21)	NS
60-69	58 (43)	45 (34)	67 (49)	170 (42)	
70-79	35 (26)	48 (36)	39 (28)	122 (30)	
80-	12 (9)	12 (9)	6 (4)	30 (7)	
Mean ± SD	67 ± 9	68 ± 9	66 ± 8		
Time after menopause (years)					
-9	22 (18)	22 (17)	21 (16)	65 (17)	NS
10-19	47 (38)	33 (26)	58 (44)	138 (36)	
20-	54 (43)	68 (54)	52 (39)	174 (45)	
Unknown	2 (2)	3 (2)	1 (1)	6 (2)	
Mean ± SD	18 ± 8 or 9	20 ± 10	18 ± 9		
Body weight (kg)					
-39	12 (9)	16 (12)	17 (12)	45 (11)	NS
40-49	55 (41)	54 (41)	49 (36)	158 (39)	
50-59	48 (36)	54 (41)	54 (39)	156 (38)	
60-	20 (15)	9 (7)	18 (13)	47 (12)	
Mean ± SD	50 ± 8	48 ± 8	49 ± 8		

Subjects were divided into three groups after the initial exclusion of 8 subjects from the original 414 with percentages in parentheses according to the intention-to-treat principle
NS, no significant difference

Table 4. Bone-related pre-study background data in the subjects at start divided into three groups

Group	A	B	C	Total	Results of statistical analysis
Number of subjects at start	135	133	138	406	
Number of spinal fractures					
0	77 (57)	63 (47)	67 (49)	207 (51)	NS
1	26 (19)	28 (21)	30 (22)	84 (21)	
2	16 (12)	12 (9)	12 (9)	40 (10)	
3	3 (2)	9 (7)	9 (7)	21 (5)	
4	5 (4)	7 (5)	3 (2)	15 (4)	
5	3 (2)	4 (3)	4 (3)	11 (3)	
6 or more	4 (3)	8 (6)	11 (8)	23 (6)	
Unknown	1 (1)	2 (2)	2 (1)	5 (1)	
BMD L2-L4 (QDR equivalent) (g/cm^2)					
Mean ± SD	0.717 ± 0.131	0.714 ± 0.127	0.716 ± 0.133		NS

Percentages are shown in parentheses according to the intention-to-treat principle
BMD, bone mineral density

Table 5. Background laboratory data in the three groups

Group		A	B	C	Results of statistical analysis
Number of subjects at start		135	133	138	
Serum Ca (mg/dl)		9.19 ± 0.49	9.24 ± 0.52	9.16 ± 0.53	NS
Serum P (mg/dl)		3.51 ± 0.48	3.58 ± 0.54	3.52 ± 0.49	NS
Serum Alkaline Phosphatase	(IU)	183.7 ± 77.9	189.3 ± 95.6	183.4 ± 74.7	NS
	(KA)	7.43 ± 1.95	7.61 ± 2.35	8.01 ± 2.76	
	(BL)	4.11 ± 2.83	3.49 ± 1.94	2.92 ± 1.05	
Urinary Ca/Cr		0.21 ± 0.14	0.23 ± 0.14	0.21 ± 0.14	NS
Urinary P/Cr		0.66 ± 0.37	0.69 ± 0.32	0.67 ± 0.36	NS
Urinary hydroxyproline/Cr		0.022 ± 0.014	0.024 ± 0.020	0.022 ± 0.011	NS
Parathyroid hormone (PTH) (pg/ml)		455.1 ± 195.2	449.5 ± 204.8	451.2 ± 181.7	NS
Serum osteocalcin (ng/ml)		8.24 ± 4.23	8.64 ± 4.88	8.47 ± 4.37	NS
Serum 1,25(OH) vitamin D (ng/ml)		52.19 ± 29.01	52.67 ± 21.07	49.55 ± 17.45	NS
Serum 25(OH) vitamin D (ng/ml)		21.42 ± 7.59	21.91 ± 7.39	21.82 ± 7.30	NS

Date are mean ± SD according to the intention-to-treat principle

Table 6. Rate of change of DXA Values (% change): intention-to-treat (ITT) analysis using constant figures to fill the defective sites

Method	Treatment	Number of cases	Mean (%)	SD	*P* values on signed-rank test
ITT	EHDP 200 mg	137	2.527	4.814	<0.0001
	EHDP 400 mg	137	3.639	5.861	<0.0001
	Alfacalcidol 1 μg	140	−0.336	4.286	0.3295
Original data	EHDP 200 mg	104	1.918	4.327	<0.0001
	EHDP 400 mg	110	2.921	5.445	<0.0001
	Alfacalcidol 1 μg	103	−0.255	3.728	0.3295

Final data consisted of last observation carried forward (LOCF)
EHDP, etidronate

Table 7. Logistic procedure on incident fractures (Fx)

		Whole series	Fx (−) at start	Fx (+) at start
Odds ratio (confidence interval)	EHDP 200 mg	0.4441 (0.1921–1.026)	0.4031 (0.1598–1.0176)	0.5534 (0.1960–1.5025)
	EHDP 400 mg	0.3466 (0.1420–0.8464)	0.3097 (0.1172–0.8181)	0.4959 (0.1679–1.4645)

Significant range is underlined

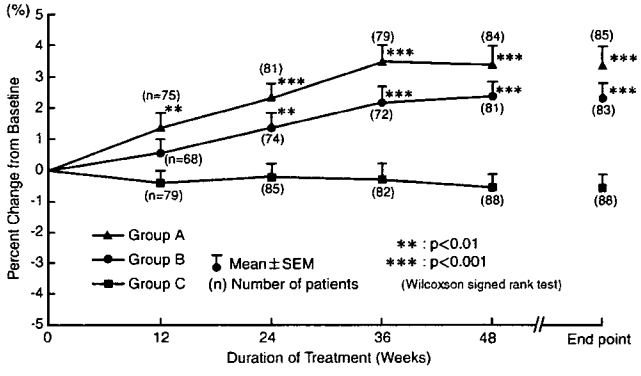

Fig. 1. Percent (%) changes of the lumbar spine bone mineral density (BMD) L2–L4 from baseline during the trial period (*vertical axis*) and duration of treatment in weeks (*horizontal axis*). Values for Group A at 12 weeks and subsequently those for Group B at 24 weeks and subsequently were both significantly higher from the baseline, whereas those for Group C did not change at any time, without a significant difference from baseline

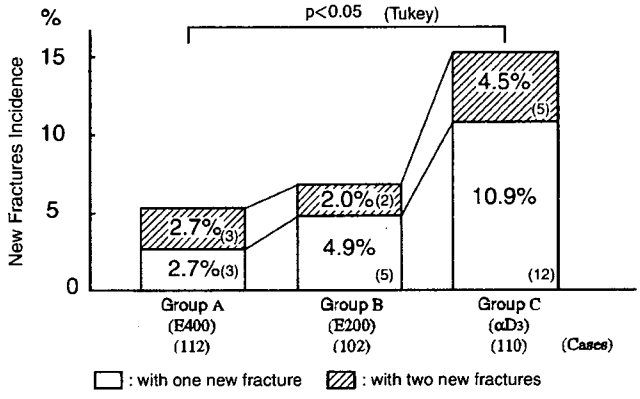

Fig. 2. Incident vertebral fracture during the test period. In Group C, one fracture occurred in 10.9% and two fractures in 4.5%; in Group A, the corresponding values were 2.7% and 2.7%, respectively, significantly lower than the former by the Tukey test; and in Group B, the corresponding values were 4.9% and 2.0%

Group C ($P < 0.001$). The results of intention-to-treat analysis on lumbar spine BMD are summarized in Table 6. Significant increase was noted in both groups given etidronate. Figure 2 illustrates new fracture in patients with one new vertebral fracture and those with multiple new vertebral fractures. In 10.9 and 4.5% of Group C, one and two new spinal fractures, respectively, occurred during the trial period, whereas such fractures occurred only in 2.7 and 2.7% of Group A and 4.9 and 2.0% of Group B.

Logistic analysis of incident fracture is summarized in Table 7. Significant reduction was noted only in the group given 400 mg etidoronate, in the whole series, and the group without prevalent fracture at the start of the study. The difference between Groups A and C was significant at $P < 0.05$ by the Tukey test. These patients were separated into those without fracture at entry and those with fracture at entry (Fig. 3). Among those without fracture at entry, one fracture occurred in 8.5% and two fractures in 1.7% of Group C, but none occurred in Groups A and B. The difference in fracture incidence between Groups A and C was significant at $P < 0.01$ and that between Groups B and C at $P < 0.05$. Among those with fracture at the beginning, 13.7% of Group C sustained one new fracture and 7.8% more than two, and the corresponding figures were 6.0 and 6.0% in Group A and 9.4 and 3.8% for Group B; however, the differences among the three groups were not significant.

In all the three groups, backache improved compared to the baseline level after 4 weeks. After 12 weeks, the cumulative rate of improvement reached 20%, and Groups A and B showed better results than in Group C (Fig. 4).

Changes of biochemical markers of bone turnover are shown in Fig. 5. Urinary hydroxyproline/Cr, a bone resorption marker, tended to fall in all three groups, especially in Group A (Fig. 5). Two bone formation markers showed

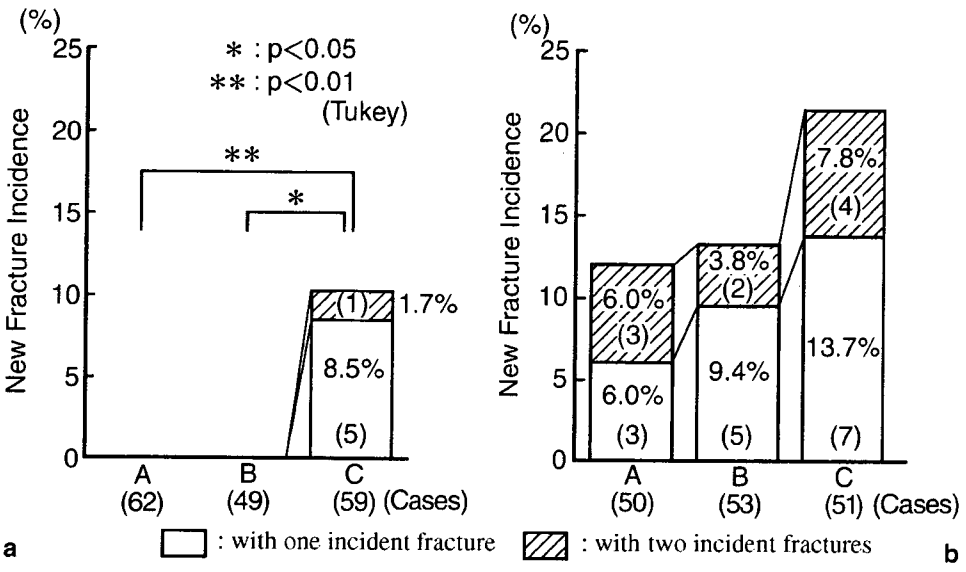

Fig. 3. Patients analyzed in Fig. 4 were divided into (**a**) those without prevalent fracture at entry and (**b**) those with prevalent fractures at entry. **a** One fracture occurred in 8.5% and two fractures in 1.7% in Group C, whereas no fractures occurred in Groups A and B. **b** One fracture occurred in 13.7% and two fractures in 7.8% in Group C; the corresponding figures were 6.0% and 6.0% in Group A and 9.4% and 3.8% in Group B, with less remarkable difference among the three groups. In subjects without prevalent fracture at entry, incident fracture occurred significantly less frequently in Group A ($P < 0.01$) and in Group B ($P < 0.05$) than in Group C by the Tukey test

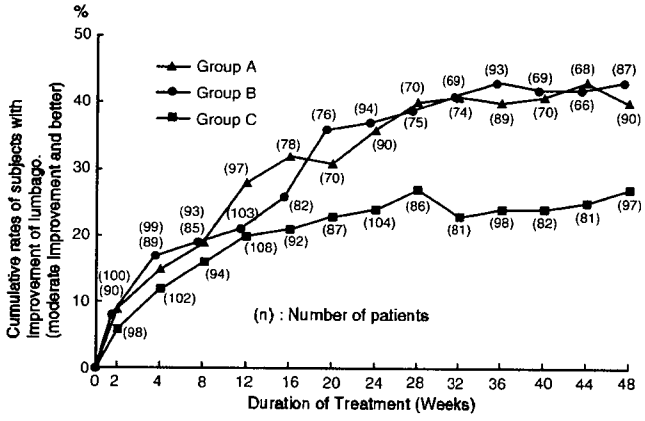

Fig. 4. Cumulative rates of definite improvement of backache: cumulative percentages of subjects with improvement of lumbago (*vertical axis*) and duration of treatment in weeks (*horizontal axis*). Group A and B gave higher values than Group C at 24 weeks

Table 8. Side effects shown according to the intention-to-treat principle

Group	A	B	C
Number of patients	135	133	138
Patients with side effects	14	8	10
Episodes of side effects	18	11	13
Gastrointestinal episodes	12	9	6
Oral episodes	4	1	0
Dermal episodes	1	1	1
Electrolyte imbalance	1	0	3
Others	0	0	3

different transitions; serum alkaline phosphatase fell from the preadministration level in all groups, especially markedly in Group A (Fig. 5), and serum osteocalcin fell progressively in Group A, followed by Group B, throughout the trial, but stayed almost unchanged in Group C (Fig. 5). Serum calcium showed a transient fall in Group A after 12 weeks but stayed within the normal range in all other groups. Serum P showed transient rises in all groups after 4 weeks, but returned to the normal range thereafter. Serum PTH showed a significant fall from the preadministration level after 12 weeks in Group C, but stayed within the normal range in Groups A and B, with a tendency for a slight rise toward the end of the trial. Urinary Ca/Cr ratio and P tended to rise in Group C, but stayed almost constant, except for mild transient falls, in Groups A and B.

Side effects are summarized in Table 8. Some side effects were seen in 14 of 135 patients in Group A, 8 of 133 in Group B, and 10 of 138 in Group C. Gastrointestinal side effects were seen most frequently, and others were rather infrequent, without remarkable difference among the three groups.

Discussion

Etidronate, 200 or 400 mg daily for 2 weeks followed by a 10-week interval, repeated in four cycles, significantly increased spinal BMD measured by DXA over the basal level and also above the level maintained by daily administration of 1 μg alfacalcidol throughout the 48 weeks of the trial. New occurrence of spinal fracture deformity was also reduced by the administration of cyclic administration of 200 or 400 mg etidronate from the level obtained by the administration of alfacalcidol, especially in those without spinal fracture at the beginning of the trial.

The effect of etidronate to increase bone density has been reported in several prospective controlled studies [18–20], but the effect on spinal fracture incidence has been rather controversial. Alfacalcidol was also reported to increase BMD and to reduce the number of spinal fracture significantly better than inactive placebo. No inactive placebo was used in the present study because it was thought that 48 weeks was too long a period to maintain osteopo-

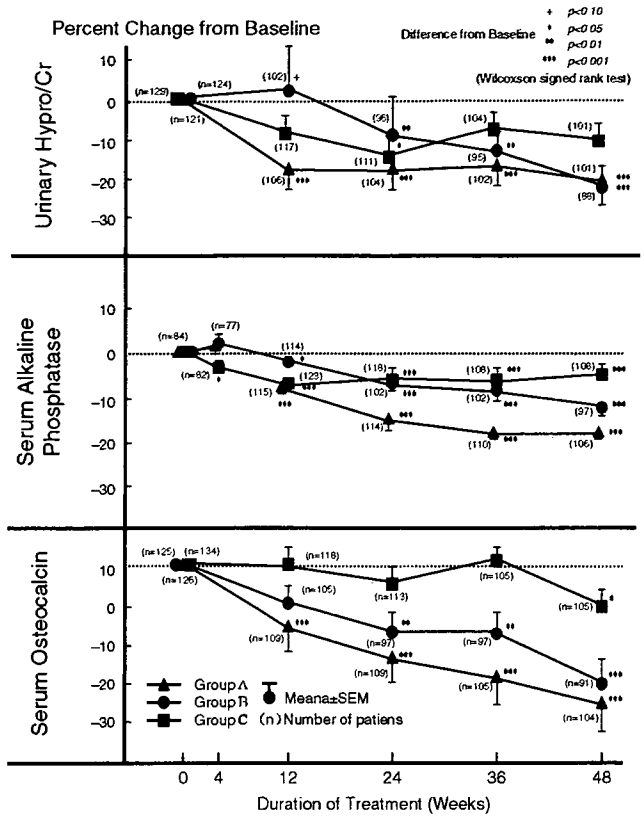

Fig. 5. *Top*: Urinary hydroxyproline/Cr (*vertical axis*) relative to duration of treatment in weeks (*horizontal axis*). A significant decrease of urinary hydroxyproline/creatinine ratio from the baseline value was noted after 12 weeks of treatment in Group A and after 24 weeks of treatment in Group C and Group B by Wilcoxon's signed rank test ($P < 0.0001$). *Middle*: On the *vertical axis* is shown percent serum alkaline phosphatase and on the *horizontal axis* duration of treatment in weeks. A significant decrease of alkaline phosphatase was already noted after 4 months of treatment in Group C ($P < 0.05$). After 12 months of treatment, a highly significant decrease was noted in Groups A and B ($P < 0.0001$), and a significant difference was also noted in Group C. Decreases persisted thereafter in all groups. *Bottom*: Serum osteocalcin (*vertical axis*) and duration of treatment (*horizontal axis*). A highly significant decrease of serum osteocalcin was already noted after 12 months of treatment in Group A, but not in Groups B and C; after 24 months, a significant decrease was noted in Groups A and B. In Group C, it was not until after 48 weeks that a slight but significant decrease appeared

rotic patients on an inactive placebo. Alfacalcidol was shown to maintain BMD, at least at the pretrial level, whereas age-related decrease of bone density was otherwise expected. Because cyclic etidronate therapy for 2 weeks on and 10 weeks off at 200 or 400 mg per day gave a significantly higher BMD and lower incidence of spinal fracture, etidronate appeared to be a useful drug to inhibit the progress of osteoporosis in this group of patients. The mean age of the patients who participated the study was 67, beyond the so-called immediate postmenopausal range and higher than that in most of the previous studies, which may add some significance to this study in enlarging the range of osteoporotic patients treated with this drug in addition to the genetic and nutritional differences. Calcium intake by Japanese, 500–550 mg/day, for instance, is generally lower than ordinary intake by Westerners. The cumulative rate of good responders to treatment as to backache suggested a more favorable response to 400 mg etidronate than 200 mg etidronate or alfacalcidol, especially after 6 months of treatment.

As a limitation of the present study, admission criteria for the study were rather complex because of the concern about nonosteoporotic bone disease. The number of subjects for DXA data analysis became unexpectedly smaller because of degenerative changes of the spine in greater age. The design of the study, involving prospective double-blind control, made a long-term continuation of more than 48 weeks difficult. The proposed duration of the present study, 48 weeks, was thought to be too short to provide sufficient data allowing accurate analysis of the frequency of incident fracture. Lumbar BMD was therefore chosen as the primary endpoint. Further studies of longer duration are desirable to provide more definite evidence of the effect of etidronate on incident fracture, especially because of the rather unexpectedly favorable findings in the present study.

Acknowledgments The loss of two original coauthors is deeply regretted. Dr. Masaaki Fukase of Kobe University passed away in March 1995, immediately after the Kobe earthquake. Dr. Hirotoshi Morii, Professor Emeritus, Osaka City University, passed away on April 6, 2006. This double-blind clinical test was supported by Dainippon Sumitomo Pharma, Osaka, Japan, with Dr. Y. Shimakoshi as the coordinator. The cooperation of Chugai Pharmaceutical Co., Ltd. and Procter & Gamble Pharmaceuticals is also appreciated. The following 36 centers participated the study: Hokkaido University (Orthopedic Surgery), Bibai Rosai Hospital (Orthopedic Surgery), Shin-Sapporo Orthopedic Hospital (Orthopedic Surgery), Eniwa Hospital (Orthopedic Surgery), Tohoku University (Orthopedic Surgery), The University of Tokyo (Geriatrics, Orthopedic Surgery, and Orthopedic Surgery of the University of Tokyo Hospital Branch), Kyorin University (Orthopedic Surgery), Tokyo Metropolitan Rehabilitation Hospital (Orthopedic Surgery), Yamanashi Medical College (Orthopedic Surgery), Hamamatsu University (Orthopedic Surgery), Aobadai Fukuchi Orthopedic Surgical Hospital, Toyama Medical and Pharmaceutical University (Orthopedic Surgery), Shakaihoken Takaoka Hospital (Orthopedic Surgery), Aichi Medical University (Clinical Laboratories), Hachiya Orthopedic Surgical Hospital, Shiga University of Medical Science (Radiology and Nuclear Medicine), Takashima Grand Hospital, Kyoto Municipal Hospital (Internal Medicine), Osaka City University (Second Department of Internal Medicine), Hoshigaoka Kouseinenkin Hospital (Orthopedic Surgery), Aijinkai Takatsuki Hospital (Internal Medicine), Komatsu Hospital (Orthopedic Surgery), Kobe University (Third Division, Department of Medicine), Hyogo College of Medicine (Orthopedic Surgery), Okayama University (Orthopedic Surgery), Kawasaki Medical School (Nuclear Medicine), Okayama City Hospital (Orthopedic Surgery), Tottori University (Orthopedic Surgery), San-in Rosai Hospital (Orthopedic Surgery), Kagawa Medical College (Orthopedic Surgery), Spine Injury Center (Orthopedic Surgery), Kurume University (Orthopedic Surgery), Nagasaki University (First Department of Internal Medicine and Orthopedic Surgery), and University of the Ryukyus (Orthopedic Surgery).

References

1. Sato M, Graser W (1990) Effect of bisphosphonates on isolated rat osteoclasts as examined by reflected light microscopy. J Bone Miner Res 5:31–40
2. Carano A, Teitelbaum SL, Konsek JD, Schlesinger PH, Blair HC (1990) Bisphosphonates directly inhibit the bone resorption activity of isolated avian osteoclasts in vitro. J Clin Invest 85:456–461

3. Hughes DE, MacDonald RR, Russell RGG, Gowen M (1989) Inhibition of osteoclasts-like cell formation by bisphosphonate in long term culture of human bone marrow. J Clin Invest 83:1930–1935
4. Heaney RP, Saville PD (1976) Etidronate disodium in postmenopausal osteoporosis. Clin Pharmacol Ther 20:593–604
5. Gennari C (1980) Disodium etidronate treatment of osteoporosis. In: Caniggia A (ed) Proceedings of the First International Symposium on Diphosphonate in Therapy, Pisa, Italy. Via Mazzini, Pisa, pp 133–146
6. Watts NB, Harris ST, Genant HK, Wasnich RD, Miller PD, Jackson RD, Licata AA, Ross P, Woodson GC III, Yanover MJ (1990) Intermittent cyclical etidronate treatment of postmenopausal osteoporosis. N Engl J Med 323:73–79
7. Cranney A, Guyatt G, Krolicki N, Welch V, Griffith L, Adachi JD, Shea B, Tugwell P, Wells G; Osteoporosis Research Advisory Group (ORAG) (2001) A meta-analysis of etidronate for the treatment of postmenopausal osteoporosis. Osteoporos Int 12:140–151
8. Ott SM, Woodson GC, Huffer WE, Miller PD, Watts NB (1994) Bone histomorphometric changes after cyclic therapy with phosphate and etidronate disodium in women with postmenopausal osteoporosis. J Clin Endocrinol Metab 78:968–972.
9. Hasling C, Charles P, Jensen FT, Mosekilde L (1994) A comparison of the effects of oestrogen/progestogen, high-dose oral calcium, intermittent cyclic etidronate and an ADFR regime on calcium kinetics and bone mass in postmenopausal women with spinal osteoporosis. Osteoporos Int 4:191–203
10. Miller PD, Watts NB, Licata AA, Harris ST, Genant HK, Wasnich RD, Jackson PD, Hoseyni MS, Schoenfeld SL, Valent DJ, Chesnut GH III (1997) Cyclical etidronate in the treatment of postmenopausal osteoporosis: efficacy and safety after seven years of treatment. Am J Med 103:468–476
11. Fujita T (1992) Vitamin D in the treatment of osteoporosis. Proc Soc Exp Biol Med 199:394–399
12. Orimo H, Shiraki M, Hayashi Y, Nakamura T (1987) Reduced occurrence of vertebral fracture in senile osteoporosis treated with 1-alpha(OH) vitamin D_3. Bone Miner 3:47–52
13. Papadimitropoulos E, Wells G, Shea B, Gillespie W, Weaver B, et al; Osteoporosis Methodology Group and The Osteoporosis Research Advisory Group (2002) Meta-analyses of therapies for postmenopausal osteoporosis. VIII: Meta-analysis of the efficacy of vitamin D treatment in preventing osteoporosis in postmenopausal women. Endocr Rev 23:560–569
14. De Leenheer AP, Bauwens RM (1985) Comparison of a cytosol radioreceptor assay with a radioimmunoassay for 1,25-dihydroxyvitamin D in serum or plasma. Clin Chim Acta 152: 143–154
15. Haddad JG, Chyu KJ (1971) Competitive protein-binding radioassay for 25-hydroxycholecalciferol. J Clin Endocrinol Metab 33:992–995
16. Slatopolsky E, Martin K, Morrissey J, Hruska K (1982) Current concepts of the metabolism and radioimmunoassay of parathyroid hormone. J Lab Clin Med 99:309–316
17. Sone T, Tomomitsu T, Fukunaga M (1995) Standardization of diagnosis with various dual X-ray absorptiometry systems (in Japanese). Osteoporosis Jpn 3:223–225
18. Jowsey J, Riggs BL, Kelly PJ, Hoffman DL, Bordier P (1971) The treatment of osteoporosis with disodium ethene-1,1-diphosphonate. J Lab Clin Med 78:574–584
19. Volkema R, Vismans F-J, Papapoulos SE, Pauwels EK, Bijvoet OLM (1989) Maintained improvement in calcium balance and bone mineral content in patients with osteoporosis treated with the bisphosphonates APD. Bone Miner 5:183–192
20. Storm T, Thamsborg C, Steiniche T, Genant HK, Soerensen OH (1990) Effect of intermittent cyclical etidronate therapy on bone mass and fracture rate in women with postmenopausal osteoporosis. N Engl J Med 322:1265–1271

Local Application of Recombinant Human Fibroblast Growth Factor-2 on Bone Repair: A Dose–Escalation Prospective Trial on Patients with Osteotomy

Hiroshi Kawaguchi,[1] Seiya Jingushi,[2] Toshihiro Izumi,[3] Masao Fukunaga,[4] Takashi Matsushita,[5] Takashi Nakamura,[6] Kosaku Mizuno,[7] Toshitaka Nakamura,[8] Kozo Nakamura[1]

[1]Sensory & Motor System Medicine, University of Tokyo, Hongo 7-3-1, Bunkyo, Tokyo 113-8655, Japan

[2]Kyushu University, Fukuoka 812-8582, Japan

[3]Saihaku Hospital, Tottori 683-0323, Japan

[4]Kawasaki Medical School, Okayama 701-0192, Japan

[5]Teikyo University, Tokyo 173-8606, Japan

[6]Kyoto University, Kyoto 606-8507, Japan

[7]Kobe Rosai Hospital, Hyogo 651-0053, Japan

[8]University of Occupational and Environmental Health, Fukuoka 807-8555, Japan

Received 28 December 2005; accepted 4 August 2006

Published online 4 January 2007 in Wiley InterScience (www.interscience.wiley.com). DOI 10.1002/jor.20315

ABSTRACT: Based on preclinical evidence in animal models, the present study examined the clinical efficacy and safety of recombinant human fibroblast growth factor-2 (rhFGF-2) to accelerate bone repair in a dose-escalation prospective trial. One of three dosages (200, 400 or 800 μg) of rhFGF-2 in a biodegradable gelatin hydrogel was injected during surgery into the osteotomy site of 59 knee osteoarthritis patients undergoing high tibial osteotomy, and 57 of them were monitored for 16 weeks. The rhFGF-2 dose dependently increased the percentage of patients with radiographic bone union, and decreased the average time needed for such union. The percentages of patients with an absence of pain and full-weight bearing were also greater in the higher dosage groups than in the low dosage group, especially in the clinically critical periods 6, 8, and 10 weeks. Neither blood chemistries nor clinical adverse events were associated with the rhFGF-2 dosages. We therefore conclude that the rhFGF-2 in gelatin hydrogel dose dependently accelerated radiographic bone union of a surgical osteotomy with a safety profile at least at the dosages used, suggesting the clinical efficacy of this agent for bone repair. © 2007 Orthopaedic Research Society. Published by Wiley Periodicals, Inc. J Orthop Res 25:480–487, 2007

Keywords: fibroblast growth factor; fracture; bone; human

INTRODUCTION

Development of synthetic materials with osteogenic properties is a major goal of the orthopedic research field. Because growth factors are expressed during various phases of bone repair, there has been considerable interest in their use as therapeutic agents to enhance the repair in accordance with the recent advent of their recombinant proteins.[1] Fibroblast growth factors (FGFs) are a family of 23 structurally related polypeptides that are characterized by their affinity for the glycosaminoglycan heparin-binding sites on cells, and are known to play a critical role in angiogenesis and mesenchymal cell mitogenesis.[2] The most abundant FGFs in normal adult tissue are fibroblast growth factor-1 (FGF-1 or acidic FGF) and FGF-2 (basic FGF), both of which have been identified during the early stages of bone repair, although FGF-2 is a more potent mitogen than FGF-1.[3] In skeletal tissues, FGF-2 is accumulated in bone matrix and acts as an autocrine/paracrine factor.[4] Several genetic diseases with abnormalities in bone and cartilage formation, such as achondroplasia and thanatophoric dysplasia type II, have been shown to be due to mutations of genes for FGFs or their receptors,[5] suggesting the importance of FGFs in bone and

Correspondence to: Hiroshi Kawaguchi (Telephone: (+81)-33815-5411 (ext. 33376); Fax: (+81)-33818-4082; E-mail: kawaguchi-ort@h.u-tokyo.ac.jp)

cartilage formation. We and others have reported the anabolic effect of local and systemic administrations of FGF-2 on bone formation using several animal models including nonhuman primates.[6–15] A single local application of FGF-2 facilitated the healing of bone fracture and segmental bone defect in normal and diabetic rats, rabbits, dogs, and monkeys;[6–12] stimulated bone formation in callotasis bone lengthening in rabbits;[13] and increased bone mass intraosseously in normal and ovariectomized rats and rabbits.[14] In addition, a daily systemic administration of FGF-2 facilitated endosteal bone formation.[15] Regarding the delivery system for clinical use, previous animal studies have revealed that FGF-2 exerted the most potent anabolic activity when a synthetic bioabsorbable hydrogel prepared through glutaraldehyde crosslinking of gelatin was used as the carrier.[11,16,17] Based on these preclinical studies, the present study for the first time evaluated the efficacy and safety of the use of recombinant human fibroblast growth factor-2 (rhFGF-2) in the biodegradable gelatin hydrogel for bone repair in a clinical dose–escalation trial.

MATERIALS AND METHODS

Materials

rhFGF-2 was provided by Kaken Pharmaceutical Co., Ltd. (Tokyo, Japan). Biodegradable gelatin hydrogel was prepared through the glutaraldehyde crosslinking of acidic gelatin that was purified from natural bovine bone, as reported previously.[16,17]

Study Design

The present study was designed with a reasonable sample size as the first exploratory trial that examined the effects of rhFGF-2 administration in humans with safety and accuracy. Between November 2000 and March 2004, 59 patients (40–74 years old) with osteoarthritis in the medial compartment of the knee, who were planning to undergo closing wedge high tibial osteotomy, were enrolled for this dose–escalation trial at 16 medical centers and hospitals in Japan. Exclusion criteria included use of medications that were known to affect bone and cartilage metabolism (e.g., bisphosphonates, vitamin D derivatives, calcitonin, vitamin K_2, ipriflavone, estrogen, androgen, calcium supplement, corticosteroids), osteoporosis, diabetes, malignant tumor, and prior surgery on bone or joint. Pain medications were not restricted, and all patients used nonsteroidal anti-inflammatory drugs (NSAIDs) before or during the observation period, although the duration was not significantly different among the groups. After approval of the protocol by the Institutional Review Boards (IRB) at all participating institutions and after the patients had provided written informed consent, patients were assigned in order of enrollment to one of three investigational groups that received a total dosage of 200, 400, or 800 μg of rhFGF-2 in a biodegradable gelatin hydrogel carrier (the total reconstituted volume was 1 mL). The rhFGF-2 dosages were determined based on previous preclinical results of osteotomy experiments on rats, rabbits, dogs, and monkeys[7–9,12] through normalizing by the cross section area of the bones. Safety of a dosage was assessed and confirmed before proceeding to a higher trial dosage. For the surgery, through an anterior approach a closing wedge osteotomy was performed, aiming at 164–170° of postoperative femorotibial angle (FTA), with fixations by an external fixator, an internal plate or an internal staple, depending on the institution. Following wound irrigation and hemostasis, the rhFGF-2 hydrogel was injected into the osteotomy site just prior to the soft-tissue closure. A drain without suctioning was placed as far as possible from the osteomomy to avoid the potential consequences on the bioavailability of the agent.

Radiographic Assessment

Standard X-ray pictures of the anteroposterior and lateral projections were taken immediately after the surgery and at least every 2 weeks thereafter up to 16 weeks postoperatively, even if radiographic bone union was achieved at earlier time points. A panel of two orthopedic surgeons and one musculoskeletal radiologist, blinded to patient data including treatment and time following the surgery, independently assessed the presence or absence of bone union. Radiographic bone union was defined as the existence of apparent bridging by bony beam across the osteotomy gap on anteroposterior and lateral projections in patients with external and internal staple fixations, and on anteroposterior projection in those with internal plate fixation.

Clinical Assessment

Clinical assessment included the presence of pain at the osteotomy site and the ability for full weight-bearing on the operated leg. Although neither NSAIDs nor analgesics were restricted during the observation period, pain free was defined as no pain at the osteotomy site during daily activities without the pain medications. From 6 weeks after surgery, as much weight bearing as possible was allowed unless the patient felt pain while walking. In addition, clinical healing was defined as both the radiographic bone union and the absence of pain at the osteotomy site. These criteria were evaluated every 2 weeks up to 16 weeks, even if there was no clinical problem at earlier time points.

Blood Chemistries

The serum calcium and phosphate levels were measured by orthocresolphthalein complexone and direct molybdic method, respectively (SRL Inc., Tokyo, Japan), preoperatively, and 2 and 4 weeks postoperatively. The calcitonin and osteocalcin levels were measured by

radioimmunoabsorbent assay (RIA; SRL Inc.). The serum level of FGF-2 was monitored by enzyme-linked immunoabsorbent assay (ELISA; Kaken Pharmaceutical Co., Ltd., Tokyo) before and 2, 4, 24, and 2 weeks after the surgery. All patients were also screened for antibodies to FGF-2 and gelatin preoperatively and 2 and 4 weeks postoperatively, by ELISA (Kaken Pharmaceutical Co., Ltd.) and fluorescence enzyme immunoabsorbent assay (FEIA; SRL Inc.), respectively.

Safety Assessment

Safety was monitored according to the number and duration of adverse events. An adverse event was defined as any local or systemic sign, symptom, syndrome, illness, medical condition, or abnormal laboratory data that occurred or worsened after surgery, regardless of causality or treatment group. Infections were conservatively defined as any suspected or confirmed superficial or deep bone or soft-tissue infection, with or without bacteriological confirmation. Retrospectively, all adverse events were classified as serious or nonserious according to ICH Guidelines (International Conference of Harmonization Guideline Clinical Safety Data Management: Definitions and Standards for Expedited Reporting. Federal Register, March 1, 1995).

Statistical Analyses

Baseline characteristics of patients were tested using one-way analysis of varience (ANOVA) or Fisher's exact test. Dose response effects among three dosages of rhFGF-2, and pair-wise comparisons were evaluated by generalized Wilcoxon test and Tukey-Kramer method, respectively. Differences in the number and duration of adverse events were evaluated by Fisher's exact test. Comparison of the serum concentrations was performed with one-way ANOVA and paired t-test. A p-value of <0.05 for analysis of safety variables was considered significant. Data analyses were performed using SAS version 8.0 (SAS Institute Inc., Cary, NC).

RESULTS

Demographics

Fifty-nine patients were enrolled from 16 institutions, and two patients (one for spontaneous retraction of the informed consent and the other for the onset of heart failure) were withdrawn, so that investigations were performed on 57 patients (97%). There were no statistically significant differences (all $p > 0.05$) for any of the baseline data among the groups treated with 200, 400, and 800 μg of rhFGF-2 (Table 1). The low, middle, and high dosage groups consisted of 20, 18, and 19 patients with no significant difference in gender. The average age, body height, weight, and body mass index at surgery were also comparable among the three groups. Although the aimed FTA and the fixation method varied among the institutions, three was no significant difference in the corrected angle or the hardware used among the groups (all $p > 0.05$).

Radiographic Bone Union

The interrater reliability of the three independent reviewers has a weighted kappa coefficient of 0.60–0.68, suggesting an excellent reproducibility among them. All osteotomies were confirmed to show similar bone defects without radiographic

Table 1. Baseline Patient Demographics

	rhFGF-2			
	200 μg	400 μg	800 μg	p-Value
Number of patients	20	18	19	
Males/females	7/13	8/10	11/8	0.378
Age (years) (range)	62.2 ± 9.2 (41–74)	57.4 ± 6.9 (44–72)	59.7 ± 9.7 (40–71)	0.252
Height (cm) (range)	156.7 ± 8.0 (147.0–178.6)	157.1 ± 8.1 (145.8–170.0)	159.3 ± 9.4 (142.3–175.0)	0.603
Weight (kg) (range)	63.9 ± 9.6 (50.0–84.0)	68.1 ± 10.7 (51.0–88.3)	64.8 ± 9.8 (43.0–82.5)	0.415
Body mass index (kg/m^2) (range)	26.0 ± 3.2 (21.3–34.5)	27.6 ± 4.5 (22.4–36.9)	25.5 ± 2.7 (19.1–28.5)	0.167
Corrected angle (degrees)				0.847
<10	0	1	1	
10–14	10	9	7	
15–19	8	5	9	
≥20	2	3	2	
Fixation methods				0.177
External fixation	12	5	7	
Internal plate fixation	6	12	11	
Internal stabple fixation	2	1	1	

Data are mean ± SD.

DOI 10.1002/jor

bone union at time 0. The rhFGF-2 dose dependently increased the percentage of patients with radiographic bone union during the observation period up to 16 weeks ($p = 0.015$ between the high and low dosage groups; $p = 0.035$ among the three groups) (Fig. 1A). The percentages of patients with radiographic bone union in the high dosage group was about three times and twice those in the low dosage group at 8 and 10 weeks, respectively. At 12 weeks and thereafter, even the low dosage group showed radiographic bone union, and eventually at 16 weeks all patients achieved radiographic bone union. All patients with bone union at earlier time points were confirmed to conserve the status until the last visit at 16 weeks without refracture. The times needed for 50% of patients in the low, middle, and high dosage groups to show radiographic bone union were 11.5, 10.1, and 8.1 weeks, respectively (Fig. 1A). In the meantime, the average times needed for radiographic bone union in the three groups were 11.5, 9.3, and 9.0 weeks, respectively (Fig. 1B). Figure 2 shows the time course of X-ray pictures of representative patients in the three groups. In the patients of the low dosage group, the bony bridging across the osteotomy gap was not apparent even at 10 weeks. In patients of middle and high dosage groups, on the contrary, the calcified callus was observed at 6 weeks and the bony bridging at 8 weeks following the surgery.

Clinical Outcomes

We next examined the effects of rhFGF-2 on clinical outcomes. The percentages of patients who were pain free at the osteotomy site, those with full-weight bearing on the operated leg, and those with clinical healing (defined as both radiographic bone union and pain free) were higher in middle- and high-dosage groups than in the low-dosage group, especially in the clinically critical periods 6, 8, and 10 weeks after the surgery (Fig. 3). However, at 12 weeks and thereafter, even the low-dosage group showed comparable clinical outcomes to the higher groups, just like radiographic bone union. All patients deemed clinically healed at earlier time points were confirmed to have conserved that status until the last visit without recurring pain or fracture.

Blood Chemistries

The serum calcium, phosphate, calcitonin, and osteocalcin levels were measured preoperatively, and 2 and 4 weeks postoperatively. No significant

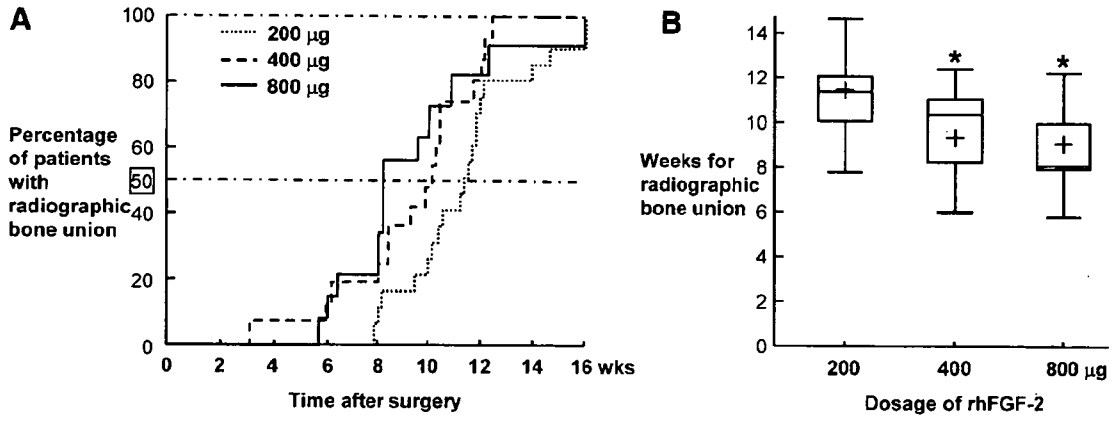

Figure 1. Comparison of radiographic bone union among patients with 200, 400, and 800 μg rhFGF-2 application. Radiographic bone union was defined as the apparent bridging by bony beam across the osteotomy gap on standard X-ray pictures that were taken immediately after the surgery and at least every 2 weeks threafter up to 16 weeks. (A) Time course of the percentage of patients with radiographic bone union during 16 weeks after the surgery in the three dosage groups. rhFGF-2 dose dependently increased the percentage of those with radiographic bone union ($p = 0.035$ among the three groups, and $p = 0.015$ between the high and low dosage groups). (B) Box and whisker plot representing weeks needed for radiographic bone union in the three dosage groups. The line through the box is the median; the top and bottom edges of each box represent the 25 and 75 percentiles, giving the interquartile range; and cross in the box is the mean. The vertical lines at each side of the box represent distribution from the quartiles to the farthest observation. *$p < 0.05$; significant difference from the 200 μg group by the Tukey-Kramer test.

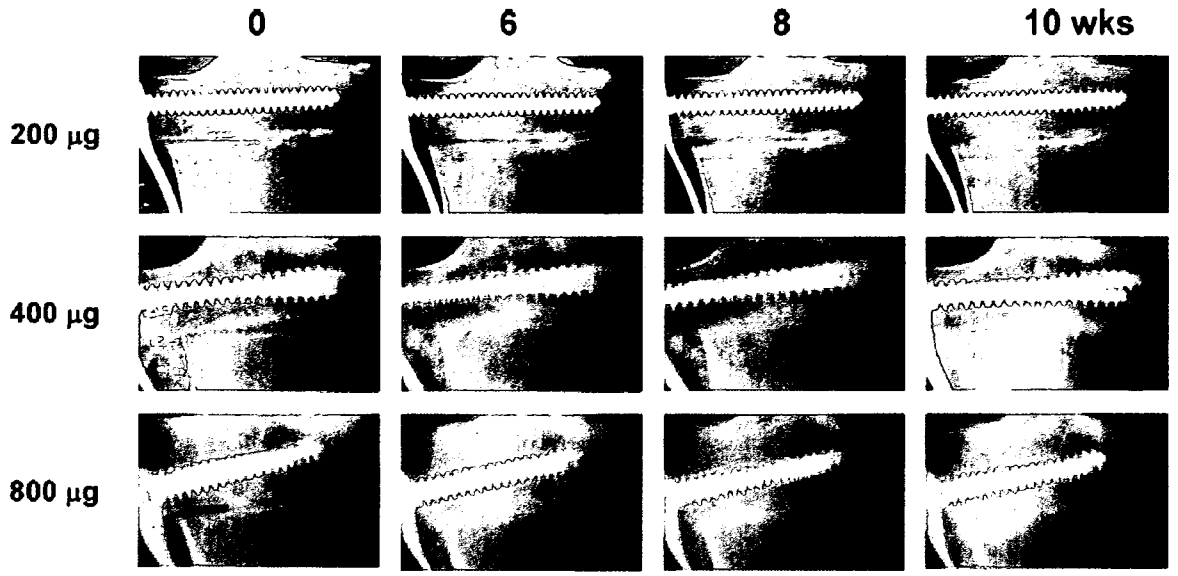

Figure 2. Anteroposterior X-ray pictures of tibial osteotomy sites of representative patients in the three dosage groups at 0, 6, 8, and 10 weeks after the surgery.

difference was detected in the calcium, phosphate, or osteocalcin levels among the three dosage groups, nor among the time points before and after the surgery (all $p > 0.05$). Although only the preoperative calcitonin level was higher in the low- dosage group, the levels became comparable after the surgery. The serum FGF-2 level also was not significantly affected by the dosage of applied rhFGF-2 at least up to 2 weeks after the application (all $p > 0.05$). Neither antibody to FGF-2 nor that to gelatin was detected in any patients preoperatively or postoperatively.

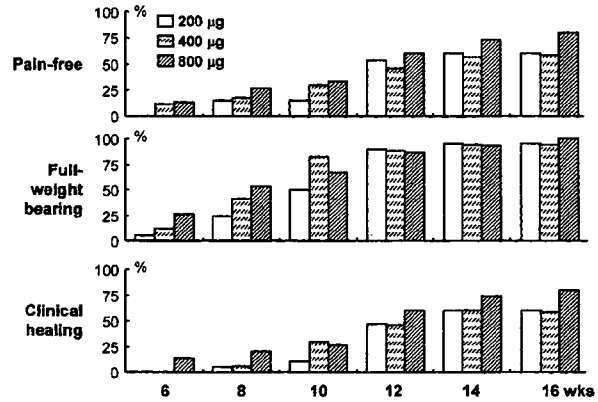

Figure 3. Comparison of clinical outcomes among patients with 200, 400, and 800 μg rhFGF-2 application. Cumulative percentage of patients with absence of pain at the osteotomy site, those with full weight bearing on the operated leg, and those with clinical healing (defined as both radiographic bone union and absence of pain) were compared every 2 weeks for 16 weeks after the surgery. The missing data of only one patient in the 400 μg group at 6 weeks were carried forward from those at 4 weeks.

Safety

The local or systemic adverse events experienced by the patients during the observation periods included several kinds of skin disorders, peroneal palsy, coryza, fever, and diarrhea (Table 2). Of the local skin disorders, the pin-site infection was most frequent and lasted 7–49 days. The durations of other systemic or local skin disorders such as eczema, eruption, and edema ranged 1–52 days. Two cases of peroneal palsy that were seen in the operated leg of the low dosage group lasted 28 and 105 days after surgery, and recovered within the obsevation period. Other systemic disorders: coryza, fever, and diarrhea were also temporary, and lasted 1–33 days. All the symptoms were classified as nonserious according to ICH Guidelines. Although the knee range of motion was not evaluated, there was no report of the disability as an adverse event. There was no case with hardware failure of the fixation device nor with heterotopic ossification of ligaments, tendons, or cartilage on X-ray during the obsevation periods. Regarding laboratory data, increases in the serum levels of C-reactive protein and fibrinogen levels may be due to the pin-infection, because both decreased to normal levels with disappearance of the infection. Slight increases in the glutamate–pyruvate–transaminase and eosinophil levels

DOI 10.1002/jor

Table 2. Adverse Events

	rhFGF-2			
	200 μg	400 μg	800 μg	Total
Local events				
Skin disorders				
Pin site infection	4	2	1	7
Eczema	0	0	1	1
Peroneal palsy	2	0	0	2
Systemic events				
Skin disorders				
Eczema	2	3	3	8
Eruption	1	1	2	4
Edema	0	0	3	3
Coryza	3	3	4	10
Fever	0	1	2	3
Diarrhea	0	0	1	1
Laboratory data				
C-reactive protein increase	2	0	1	3
Fibrinogen increase	0	0	1	1
Glutamate-pyruvate-transaminase increase	1	0	0	1
Eosinophil increase	1	0	0	1

were detected within 4 weeks after the surgery, and decreased to normal levels thereafter. All of these symptoms and abnormal laboratory data had recovered before the last visit at 16 weeks, and neither the number nor the duration statistically showed positive association with the dosages of the rhFGF-2 applied.

DISCUSSION

Based on the evidence of extensive studies using various animal models,[6–15] this study for the first time showed clinical evidence that rhFGF-2 in gelatin hydrogel accelerated radiographic bone union of the closing wedge high tibial osteotomy. Because most osteotomies can heal only with appropriate fixations, and in fact, all patients even of the low dosage group eventually achieved radiographic bone union in the present study, the rhFGF-2 application may not have yielded bone union by preventing nonunion, but just accelerated bone union. However, if the osteotomy site remains unstable for a long time, the chances of mal-union and infection causing skeletal deformity, late nerve palsy and refracture may increase. The reduction of time for bone union by the rhFGF-2 application is therefore important not only for the comfort of the patient after surgery, but also for the prevention of these secondary disorders.

FGF-2 is reported to stimulate the proliferation of immature mesenchymal cells but to inhibit the differentiation and matrix synthesis of osteoblastic cells.[18–22] Our preliminary experiments using the rat and rabbit models demonstrated that the local half-life of the injected ^{125}I-labeled FGF-2 in the gelatin hydrogel was 1 to 2 days. The percentages of the ^{125}I-labeled FGF-2 remaining localized were approximately 20, 3, and 1% at 1, 2, and 3 weeks, respectively. Hence, FGF-2 appears to have its effect primarily in the earlier stage of bone repair, probably through its mitogenic action on immature mesenchymal cells. In fact, previous animal studies demonstrated that a single injection of FGF-2 enhanced the proliferation of chondroprogenitor cells in fracture callus, causing the formation of a larger cartilage, but did not directly affect maturation of chondrocytes or replacement of the cartilage by osseous tissue.[7,14,23] Furthermore, expressions of FGF-2, FGF-1, and their principal receptor FGFR1 have been identified mainly at the early stage of fracture healing.[1,24–26] In addition to its mitogenic action on immature mesenchymal cells, FGF-2 may induce other anabolic factors such as prostaglandins, transforming growth factor (TGF)-β and bone morphogenetic proteins (BMPs), which may compose a serial cascade of bone formation. In fact, we and others have shown that FGF-2 induces TGF-β expression and prostaglandin production in a rat fracture model and in cultured osteoblastic cells.[7,27,28] Because the present blood chemistries indicate the absence of influence on systemic bone turnover and metabolism, FGF-2 may act as a local

factor that initiates the cascade of bone formation in the entire bone repair process. The follow-up period for 16 weeks might be relatively short for the safety conclusions. However, considering the above pharmacokinetics of rhFGF-2 in the gelatin hydrogel, we assume that the effect may possibly not persist after 16 weeks.

Among growth factors that have been investigated to date, BMPs appear to be the most popular that exhibit a potent osteoanabolic activity. Unlike FGF-2, BMPs strongly stimulate the differentiation and matrix synthesis of osteoprogenitor cells.[29,30] Regarding the clinical applications, three randomized trials have led to various regulatory agency approvals for specific indications of rhBMPs in the United States and other countries.[31–33] Two of them showed the positive effects on bone repair: one for rhBMP-2 on open tibial fractures[32] and the other for rhBMP-7 (rhOP-1) on tibial nonunions.[33] However, considering that as much as 12 mg of rhBMP-2 and 3.5 mg of rhBMP-7 were needed to show positive effects in those studies, bone anabolic potencies of the BMPs in clinical settings are not as impressive as those seen in animal models in which more robust bone formation and healing have been observed.[29,30] This may be because BMPs may be degraded more quickly in humans than in animals, the biology of the receptor–ligand interactions may differ, or the pharmacokinetics of the activity may be less favorable in humans.

The most important limitation of the present study is the lack of the vehicle control group (the gelatin hydrogel only). IRB of several institutions did not deem it ethically acceptable because systemic immediate-type reactions, including anaphylactic shock, to measles, mumps, rubella, and varicella vaccines reported in some children were suspected to be allergic symptoms caused by gelatin antigen that is included in the vaccines as a stabilizer.[34] The present gelatin hydrogel was therefore originally synthesized by deleting the antigenic portion.[16,17] We believe that the present result showing the absence of the antibody in the patients may lead to the approval of the clinical use of the gelatin hydrogel as the rhFGF-2 carrier. Instead of the control group, we determined the three dosages of rhFGF-2 based on previous preclinical results of osteotomy experiments on animals.[7–9,12] When the dosages in the animal studies were converted to the area of the human proximal tibiae, 800 μg of rhFGF-2 was expected to show a significant anabolic function, while 200 μg exerted little effect. In fact, the high dosage of rhFGF-2 showed significant bone anabolic function over the low dosage in the present clinical study. Furthermore, all patients of the low-dosage group also eventually achieved bone union after 16 weeks, although a previous report on the natural course of high tibial osteotomy showed that 8.5 and 5.7% remained nonunion even after 6 months and 1 year, respectively.[35] Hence, unlike BMPs, the discrepancy of bone anabolic potency between animals and humans may not be seen in the function of FGF-2. However, because the rationale for the present dose selection was not based on prior clinical evaluations to determine the dose with maximum efficacy, we are now planning a clinical trial using higher amounts of rhFGF-2.

In conclusion, the present dose–escalation clinical trial revealed that rhFGF-2 in gelatin hydrogel dose dependently accelerated bone repair of the tibial osteotomy with a safety profile. Because the formulation of the rhFGF-2 gelatin hydrogel is slightly viscid, it not only can be applied to the osteotomy site during the surgical procedure, but also can be percutaneously injected under roentgenologic guidance at the time of closed reduction of a bone fracture followed by a fixation with casting. We are now planning a more advanced clinical trial on fresh tibial fractures including a control group for the application of regulatory agency approval to obtain clinical indication of this agent. Furthermore, the development of appropriate delivery systems may yield progress; for example, a sequential delivering system of FGF-2 at the earlier stage and other differentiation factors like BMPs at the later stage might have potential as the optimal method of inducing bone formation. The extensive application of the osteoanabolic nature of FGF-2 to various skeletal disorders will be explored in the near future.

ACKNOWLEDGMENTS

This work was supported by Grants-in-Aid for Scientific Research from the Japanese Ministry of Education, Culture, Sports, Science and Technology, which had no role in study design, data collection, data analysis, data interpretation, or writing of the report. We declare that we have no conflict of interest.

REFERENCES

1. Lieberman JR, Daluiski A, Einhorn TA. 2002. The role of growth factors in the repair of bone biology and clinical applications. J Bone Joint Surg [Am] 84:1032–1044.
2. Itoh N, Ornitz DM. 2004. Evolution of the Fgf and Fgfr gene families. Trends Genet 20:563–569.
3. Canalis E, Centrella M, McCarthy T. 1988. Effects of basic fibroblast growth factor on bone formation in vitro. J Clin Invest 81:1572–1577.

DOI 10.1002/jor

4. Khan SN, Bostrom MP, Lane JM. 2000. Bone growth factors. Orthop Clin North Am 31:375–388.
5. Coumoul X, Deng CX. 2003. Roles of FGF receptors in mammalian development and congenital diseases. Birth Defects Res C Embryo Today 69:286–304.
6. Aspenberg P, Lohmander LS. 1989. Fibroblast growth factor stimulates bone formation. Acta Orthop Scand 60: 473–476.
7. Kawaguchi H, Kurokawa T, Hanada K, et al. 1994. Stimulation of fracture repair by recombinant human basic fibroblast growth factor in normal and streptozotocin-diabetic rats. Endocrinology 135:774–781.
8. Kato T, Kawaguchi H, Hanada K, et al. 1998. Single local injection of recombinant fibroblast growth factor-2 stimulates healing of segmental bone defects in rabbits. J Orthop Res 16:654–659.
9. Nakamura T, Hara Y, Tagawa M, et al. 1998. Recombinant human basic fibroblast growth factor accelerates fracture healing by enhancing callus remodeling in experimental dog tibial fracture. J Bone Miner Res 13:942–949.
10. Radomsky ML, Aufdemorte TB, Swain LD, et al. 1999. Novel formulation of fibroblast growth factor-2 in a hyaluronan gel accelerates fracture healing in nonhuman primates. J Orthop Res 17:607–614.
11. Tabata Y, Yamada K, Hong L, et al. 1999. Skull bone regeneration in primates in response to basic fibroblast growth factor. J Neurosurg 91:851–856.
12. Kawaguchi H, Nakamura K, Tabata Y, et al. 2001. Acceleration of fracture healing in non-human primates by fibroblast growth factor-2. J Clin Endocrinol Metab 86:875–880.
13. Okazaki H, Kurokawa T, Nakamura K, et al. 1999. Stimulation of bone formation by recombinant fibroblast growth factor-2 in callotasis bone lengthening of rabbits. Calcif Tissue Int 64:542–546.
14. Nakamura K, Kawaguchi H, Aoyama I, et al. 1997. Stimulation of bone formation by intraosseous application of recombinant basic fibroblast growth factor in normal and ovariectomized rabbits. J Orthop Res 15:307–313.
15. Nakamura T, Hanada K, Tamura M, et al. 1995. Stimulation of endosteal bone formation by systemic injections of recombinant basic fibroblast growth factor in rats. Endocrinology 136:1276–1284.
16. Tabata Y, Ikada Y. 1999. Vascularization effect of basic fibroblast growth factor released from gelatin hydrogels with different biodegradabilities. Biomaterials 20:2169–2175.
17. Tabata Y, Nagano A, Ikada Y. 1999. Biodegradation of hydrogel carrier incorporating fibroblast growth factor. Tissue Eng 5:127–138.
18. Hurley MM, Abreu C, Harrison JR, et al. 1993. Basic fibroblast growth factor inhibits type I collagen gene expression in osteoblastic MC3T3-E1 cells. J Biol Chem 268:5588–5593.
19. Hurley MM, Kessler M, Gronowicz G, et al. 1992. The interaction of heparin and basic fibroblast growth factor on collagen synthesis in 21-day fetal rat calvariae. Endocrinology 130:2675–2682.
20. Kato Y, Iwamoto M. 1990. Fibroblast growth factor is an inhibitor of chondrocyte terminal differentiation. J Biol Chem 265:5903–5909.
21. McCarthy TL, Centrella M, Canalis E. 1989. Effects of fibroblast growth factors on deoxyribonucleic acid and collagen synthesis in rat parietal bone cells. Endocrinology 125:2118–2126.
22. Rodan SB, Wesolowski G, Kyonggeun Y, Rodan GA. 1989. Opposing effects of fibroblast growth factor and pertussis toxin on alkaline phosphatase, osteopontin, osteocalcin and type I collagen mRNA levels in ROS 17/2.8 cells. J Biol Chem 264:19934–19941.
23. Nakajima F, Ogasawara A, Goto K, et al. 2001. Spatial and temporal gene expression in chondrogenesis during fracture healing and the effects of basic fibroblast growth factor. J Orthop Res 19:935–944.
24. Bolander ME. 1992. Regulation of fracture repair by growth factors. Proc Soc Exp Biol Med 200:165–170.
25. Bourque WT, Gross M, Hall BK. 1993. Expression of four growth factors during fracture repair. Int J Dev Biol 37: 573–579.
26. Nakajima A, Nakajima F, Shimizu S, et al. 2001. Spatial and temporal gene expression for fibroblast growth factor type I receptor (FGFR1) during fracture healing in the rat. Bone 29:458–466.
27. Kawaguchi H, Pilbeam CC, Gronowicz G, et al. 1995. Transcriptional induction of prostaglandin G/H synthase-2 by basic fibroblast growth factor. J Clin Invest 96:923–930.
28. Noda M, Vogel R. 1989. Fibroblast growth factor enhances type β1 transforming growth factor gene expression in osteoblast-like cells. J Cell Biol 109:2529–2535.
29. Einhorn TA. 2003. Clinical applications of recombinant human BMPs: early experience and future development. J Bone Joint Surg [Am] 85:82–88.
30. Luppen CA, Blake CA, Ammirati KM, et al. 2002. Recombinant human bone morphogenetic protein-2 enhances osteotomy healing in glucocorticoid-treated rabbits. J Bone Miner Res 17:301–310.
31. Burkus JK, Gornet MF, Dickman CA, et al. 2002. Anterior lumbar interbody fusion using rhBMP-2 with tapered interbody cages. J Spinal Disord Tech 15:337–349.
32. Govender S, Csimma C, Genant HK, et al. 2002. Recombinant human bone morphogenetic protein-2 for treatment of open tibial fractures: a prospective, controlled, randomized study of four hundred and fifty patients. J Bone Joint Surg [Am] 84:2123–2134.
33. Friedlaender GE, Perry CR, Cole JD, et al. 2001. Osteogenic protein-1 (bone morphogenetic protein-7) in the treatment of tibial nonunions. J Bone Joint Surg [Am] 83(Suppl):151–158.
34. Sakaguchi M, Inouye S. 2000. Systemic allergic reactions to gelatin included in vaccines as a stabilizer. Jpn J Infect Dis 53:189–195.
35. Naudie D, Bourne RB, Rorabeck CH, et al. 1999. Survivorship of the high tibial valgus osteotomy. A 10- to -22-year followup study. Clin Orthop Relat Res 367: 18–27.

Preparation and Characterization of Polyion Complex Micelles with a Novel Thermosensitive Poly(2-isopropyl-2-oxazoline) Shell via the Complexation of Oppositely Charged Block Ionomers†

Joon-Sik Park,‡ Yoshitsugu Akiyama,§ Yuichi Yamasaki,‡,∥ and Kazunori Kataoka*,‡,∥,⊥

Department of Materials Engineering, Graduate School of Engineering, The University of Tokyo, 7-3-1 Hongo, Bunkyo-ku, Tokyo 113-8656, Japan, Departments of Chemistry and Biology, University of Virginia, McCormick Road, Charlottesville, Virginia 22904, Center for NanoBio Integration, The University of Tokyo, 7-3-1 Hongo, Bunkyo-ku, Tokyo 113-8656, Japan, and Center for Disease Biology and Integrative Medicine, Graduate School of Medicine, The University of Tokyo, 7-3-1 Hongo, Bunkyo-ku, Tokyo 113-0033, Japan

Received May 22, 2006. In Final Form: September 5, 2006

Novel thermosensitive polyion complex (PIC) micelles were prepared in an aqueous medium based on the complexation of a pair of oppositely charged block ionomers, poly(2-isopropyl-2-oxazoline)-*b*-poly(amino acid)s (P*i*PrOx-*b*-PAA), containing thermosensitive P*i*PrOx segments. The controlled synthesis of P*i*PrOx-*b*-PAA was achieved via the ring-opening anionic polymerization of *N*-carboxyanhydrides (NCA) of either ϵ-benzyloxycarbonyl-L-lysine (Lys(Z)-NCA) or β-benzyl-L-aspartate (BLA-NCA) with ω-amino-functionalized P*i*PrOx macroinitiators and the subsequent deprotection reaction under acidic or basic conditions. Gel permeation chromatography (GPC) and ^{1}H NMR spectroscopy revealed that the syntheses of two block ionomers, poly(2-isopropyl-2-oxazoline)-*b*-poly(L-lysine) [P*i*PrOx-P(Lys)] and poly(2-isopropyl-2-oxazoline)-*b*-poly(aspartic acid) [P*i*PrOx-P(Asp)], proceeded almost quantitatively to give samples with a narrow molecular weight distribution ($M_w/M_n \leq 1.2$). The mixing of these two oppositely charged block ionomers in an aqueous medium led to the spontaneous formation of PIC micelles, which was confirmed by dynamic light scattering (DLS) and transmission electron microscopy (TEM). The PIC micelles were spherical particles with a narrow distribution in the range of the measured concentration (0.125−1 mg/mL) and were stable without any secondary aggregates. Furthermore, the PIC micelles had a constant cloud-point temperature (T_{cp}) of ~32 °C under physiological conditions regardless of the total concentration, suggesting that the concentration factor is almost negligible with respect to the T_{cp} of the micelles presumably because of the increased local concentration of the P*i*PrOx segments in the shell layer. These PIC micelles have a promising application as a size-regulated smart nanocontainer loading charged compounds as well as bearing a thermosensitive outer shell that is useful for physical affinity control.

Introduction

Recently, the self-assemblies of block copolymers have attracted an enormous amount of interest as potential materials in separation technology[1] and surface modification[2] and have promising carriers in drug delivery systems.[3,4] In particular, the use of polymeric micelles as drug carriers has numerous advantages[3] resulting from structural characteristics such as mesoscopic-scale size, core−shell structure, and thermodynamic stability. In particular, the polyion complex (PIC) micelles have opened the way to incorporate charged macromolecules of synthetic and biological origins, including proteins and nucleic acids, into the micelles.[5] The cores of PIC micelles could serve as nanoreservoirs for these charged compounds, allowing control of innate properties such as stability, solubility, and reactivity. A fundamental study of PIC micelle formation from a mixture of a series of oppositely charged block ionomers with poly(ethylene glycol) (PEG) as a hydrophilic segment, poly(ethylene glycol)-*b*-poly(L-lysine) [PEG-P(Lys)], and poly(ethylene glycol)-*b*-poly(aspartic acid) [PEG-P(Asp)] even revealed a unique molecular recognition process based on the length of the charged segments.[6] The PIC micelles entrapping enzymes in the core were also expected to be useful as functional materials such as nanometric-scale enzymatic reactors, which might be useful in the field of diagnostics and therapeutics.[7]

These interesting properties of PIC micelles as a functional supramolecular assembly may be enhanced when combined with a responsivity to external chemical and physical stimuli such as pH, magnetism, light, and heat. Of particular interest is the thermoresponsivity that can be a useful function in various applications including thermosensitive nanoreactors and drug delivery systems. Although there have been several studies on thermosensitive polymeric micelles with the potential to be a

† Part of the Stimuli-Responsive Materials: Polymers, Colloids, and Multicomponent Systems special issue.

* To whom correspondence should be addressed. E-mail: kataoka@bmw.t.u-tokyo.ac.jp. Tel: +81-3-5841-7138. Fax: +81-3-5841-7139.

‡ Department of Materials Engineering, Graduate School of Engineering, The University of Tokyo.

§ University of Virginia.

∥ Center for NanoBio Integration, The University of Tokyo.

⊥ Center for Disease Biology and Integrative Medicine, Graduate School of Medicine, The University of Tokyo.

(1) (a) Nagarajan, R.; Barry, M.; Ruckenstein, E. *Langmuir* **1986**, *2*, 210. (b) Hurter, P. N.; Hatton, T. A. *Langmuir* **1992**, *8*, 1291.

(2) (a) Webber, S. E. *J. Phys. Chem.* **1998**, *102*, 2618. (b) Emoto, K.; Iijima, M.; Nagasaki, Y.; Kataoka, K. *J. Am. Chem. Soc.* **2000**, *122*, 2653. (c) Otsuka, H.; Nagasaki, Y.; Kataoka, K. *Curr. Opin. Colloid Interface Sci.* **2001**, *6*, 21.

(3) (a) Kataoka, K.; Kwon, G. S.; Yokoyama, M.; Okano, T.; Sakurai, Y. *J. Controlled Release* **1993**, *24*, 119. (b) Kataoka, K.; Harada, A.; Nagasaki, Y. *Adv. Drug Delivery Rev.* **2001**, *47*, 113. (c) Nishiyama, N.; Bae, Y. S.; Miyata, K.; Fukushima, S.; Kataoka, K. *Drug Discovery Today* **2005**, 2, 21.

(4) (a) Discher, D. E.; Eisenberg. A. *Science* **2002**, *297*, 967. (b) Discher, B. M.; Hammer, D. A.; Bates, F. S.; Discher, D. E. *Curr. Opin. Colloid Interface Sci.* **2000**, *5*, 125.

(5) (a) Harada, A.; Kataoka, K. *Macromolecules* **1995**, *28*, 5294. (b) Kabanov, A. V.; Bronich, T. K.; Kabanov, V. A.; Yu, K.; Eisenberg, A. *Macromolecules* **1996**, *29*, 6797. (c) Kakizawa, Y.; Kataoka, K. *Adv. Drug Delivery Rev.* **2002**, *54*, 203.

(6) (a) Harada, A.; Kataoka, K. *Science* **1999**, *283*, 65. (b) Harada, A.; Kataoka, K. *Macromolecules* **2003**, *36*, 4995.

(7) (a) Harada, A.; Kataoka, K. *Macromolecules* **1998**, *31*, 288. (b) Harada, A.; Kataoka, K. *J. Am. Chem. Soc.* **1999**, *121*, 9241. (c) Harada, A.; Kataoka, K. *J. Am. Chem. Soc.* **2003**, *125*, 15306. (d) Jaturanpinyo, M.; Harada, A.; Yuan, X.; Kataoka, K. *Bioconjugate Chem.* **2004**, *15*, 344.

10.1021/la061431j CCC: $37.00
Published on Web 11/10/2006

Scheme 1. Syntheses of Block Copolymers (P*i*PrOx-P(Lys(Z)) and P*i*PrOx-PBLA) and Deprotected Block Ionomers (P*i*PrOx-P(Lys) and P*i*PrOx-P(Asp))

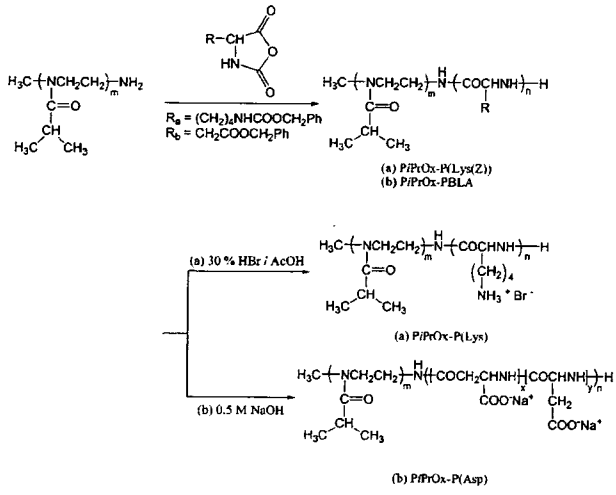

site-specific drug carrier based on poly(*N*-isopropylacrylamide) (PNIPAAm),[8] they have focused on the modulated amphiphilicity required to form the micelle with a hydrophobic inner core that is useful for the entrapment of hydrophobic therapeutic molecules such as anticancer drugs.[9] Little attention has been paid to the PIC micelles bearing a thermosensitive shell layer, though they have become even more attractive as an intelligent carrier of charged compounds utilizing temperature changes.

Of importance to the construction of PIC micelles with clear thermosensitivity are block ionomers composed of a hydrophilic segment with regulated thermosensitivity. In this regard, our recent findings of the quantitative cationic polymerization and selective end-functionalization of novel thermosensitive poly-(2-isopropyl-2-oxazoline) (P*i*PrOx) telechelics are attractive.[10] The polymerization proceeded in a good controlled manner under optimum temperature conditions with appreciably narrow molecular weight distributions ($M_w/M_n \leq 1.03$). In particular, ω-amino-terminated P*i*PrOx (Me-P*i*PrOx-NH_2) allows the synthesis of biocompatible block ionomers based on poly(amino acids) because it can serve as an efficient macroinitiator to allow the ring-opening polymerization of *N*-carboxyanhydrides of protected amino acids (NCA), including ϵ-benzyloxycarbonyl-L-lysine (Lys(Z)-NCA) and β-benzyl-L-aspartate (BLA-NCA).

In this study, we established the novel synthetic route of two kinds of block ionomers composed of P*i*PrOx as a hydrophilic segment with either the oppositely charged poly(amino acid) segment as the other block (P*i*PrOx-P(Lys) or P*i*PrOx-P(Asp)) (Scheme 1). The stable and monodispersive PIC micelles were then prepared through the electrostatic interaction between cationic (P*i*PrOx-P(Lys)) and anionic (P*i*PrOx-P(Asp)) block ionomers in an aqueous medium (Scheme 2) to explore their thermosensitive behavior under physiological conditions using the turbidimetric method. These PIC micelles may offer promising applications as a size-regulated smart nanocontainer loading charged compounds as well as bearing the thermosensitive outer shell that is useful for physical affinity control.

(8) (a) Heskins, M.; Guillent, J. E.; James, E. J. *J. Macromol. Sci. Chem.* **1968**, *A2*, 1441. (b) Schild H. G. *Prog. Polym. Sci.* **1992**, *17*, 163.

(9) (a) Cammas, S.; Suzuki, K.; Sone, Y.; Sakurai, Y.; Kataoka, K.; Okano, T. *J. Controlled Release* **1997**, *48*, 157. (b) Chung, J. E.; Yokoyama, M.; Okano, T. *J. Controlled Release* **2000**, *65*, 93.

(10) (a) Park, J. S.; Akiyama, Y.; Winnik, F. M.; Kataoka, K. *Macromolecules* **2004**, *37*, 6786. (b) Diab, C.; Akiyama, Y.; Kataoka, K.; Winnik, F. M. *Macromolecules* **2004**, *37*, 2556.

Experimental Section

Materials. 2-Isopropyl-2-oxaxoline was synthesized from isobutyric acid (Wako Pure Chemical Industries, Ltd., Japan) and 2-aminoethanol (Wako Pure Chemical) as previously described.[10] Tetrahydrofuran (THF), *n*-hexane, *N*,*N*-dimethylformamide (DMF), and chloroform (Wako Pure Chemical) were purified by distillation following conventional procedures.[11] Trifluoroacetic acid, triethylamine, and acryloyl chloride were purchased from Wako Pure Chemicals and were used without further purification. ϵ-Benzyloxycarbonyl-L-lysine and β-benzyl-L-aspartate were purchased from the Peptide Institute, Inc., Japan, and used without further purification. Bis(trichloromethyl) carbonate (triphosgene) and 30% HBr/AcOH were purchased from Tokyo Kasei Kogyo Co., Ltd., Japan, and used without further purification. The synthesis of two NCAs (ϵ-benzyloxycarbonyl-L-lysine NCA (Lys(Z)-NCA) and β-benzyl-L-aspartate NCA (BLA-NCA)) was carried out by the Fuchs–Farthing method using triphosgene.[12] α-Methyl-ω-amino-poly(2-isopropyl-2-oxazoline) (Me-P*i*PrOx-NH_2, M_n = 4500, M_w/M_n = 1.03, functionality of ω-amino group = ca. 96%) was synthesized as previously described.[10a]

Techniques. The ^{1}H NMR spectra were recorded using a JEOL EX 300 spectrometer at 300 MHz. Chemical shifts were reported in ppm downfield from tetramethylsilane. The molecular weights and molecular weight distributions were determined using a GPC (TOSOH HLC-8220) system equipped with two TSK gel columns ($G4000H_{HR}$ and $G3000H_{HR}$) and an internal refractive index (RI) detector. The columns were eluted with DMF containing lithium bromide (10 mM) at a flow rate of 0.8 mL/min and were maintained at a temperature of 40 °C. The molecular weights were calibrated with poly(ethylene glycol) (PEG) standards (Polymer Laboratories, Ltd., U.K.). The UV–vis spectra were obtained using a V-550 UV/vis Jasco spectrophotometer. Transmission electron microscopy (TEM) was performed using a Hitachi H-7000 operating at an acceleration voltage of 75 kV. Dynamic light scattering (DLS) measurements were carried out using a DLS-7000 instrument (Otsuka Electronics Co., Ltd.). Vertically polarized light at a wavelength of λ_0 = 488 nm from an Ar ion laser was used as the incident beam. The average ζ-potential and light scattering intensity at 90° (SLS mode) were measured using a Zetasizer Nano particle analyzer, NanoZS (green badge, ZEN3500; Malvern, Ltd., Malvern, U.K.) with a green laser (λ = 532 nm).

Synthesis of α-Methyl-ω-acrylate-poly(2-isopropyl-2-oxazoline) (Me-P*i*PrOx-acrylate). For comparison with the thermoresponsive behavior of Me-P*i*PrOx-OH bearing a terminal hydrophilic ω-hydroxyl group, the ω-acrylate-terminated P*i*PrOx (Me-P*i*PrOx-acrylate) was synthesized by the conversion of the ω-hydroxyl group of Me-P*i*PrOx-OH. A 53 mg (0.011 mmol) sample of Me-P*i*PrOx-OH (M_n = 4500, M_w/M_n = 1.03) was dissolved in 0.75 mL of THF with triethylamine (0.0445 g, 0.44 mmol), and acryloyl chloride (0.0195 g, 0.22 mmol) in 0.25 mL of THF was added dropwise to the solution with stirring. The reaction temperature was maintained at 0 °C. After all of the acryloyl chloride was added, the reaction was allowed to continue with stirring for 2 h at 0 °C and for 24 h at room temperature in the dark. The triethylamine hydrochloride salts were then removed by filtration. The resulting solution was dialyzed against methanol and distilled water for 48 h with periodic bath changes to remove any unreacted compounds. The final dialysis product was lyophilized overnight using a freeze dryer to give Me-P*i*PrOx-acrylate (50 mg, ca. 94% yield). The characterization of Me-P*i*PrOx-acrylate was done by MALDI-TOF mass spectrometry (M_n = 4500, M_w/M_n = 1.03, Figure S1 in Supporting Information) and ^{1}H NMR spectroscopy (the conversion efficiency is ca. 80%, Figure S2 in Supporting Information).

Synthesis of Poly(2-isopropyl-2-oxazoline)-*b*-poly(ϵ-benzyloxycarbonyl-L-lysine) Copolymer (P*i*PrOx-P(Lys(Z)) (Run 1 in Table 1). ϵ-Benzyloxycarbonyl-L-lysine NCA (Lys(Z)-NCA; 81 mg, 0.26 mmol) dissolved in 1 mL of DMF was added to a solution of α-methyl-ω-amino-poly(2-isopropyl-2-oxazoline) (Me-P*i*PrOx-NH_2,

(11) Perrin, D. D.; Armarego, W. L. F.; Perrin, D. R. *Purification of Laboratory Chemicals*; Pergamon Press: Oxford, U.K., 1980.

Scheme 2. Schematic Model of the Formation of Thermosensitive Polyion Complex (PIC) Micelles from a Pair of Oppositely Charged Block Ionomers

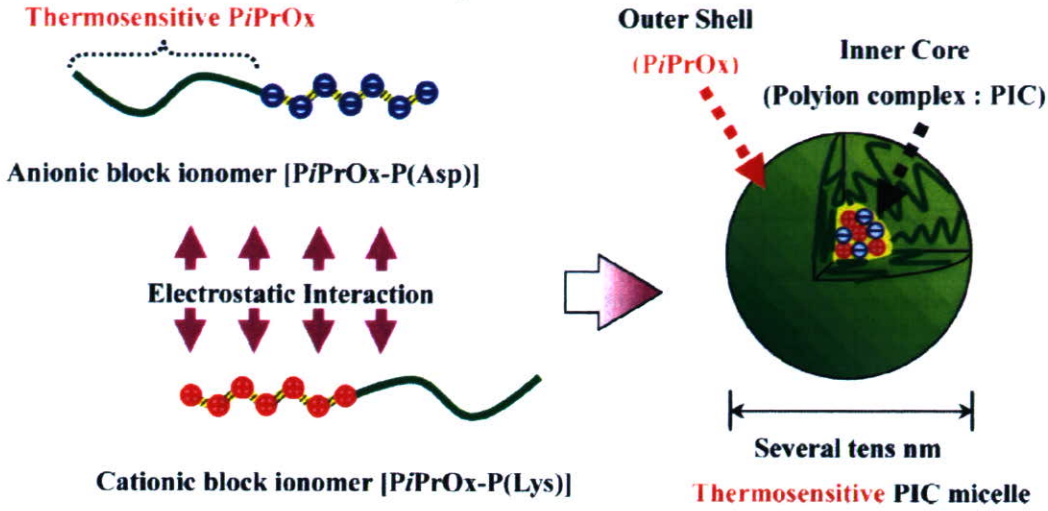

Table 1. Results of Block Copolymer Syntheses (P*i*PrOx-P(Lys(Z)) and P*i*PrOx-PBLA)

P*i*PrOx-P(Lys(Z))[a]								
macroinitiator [MI]			[Lys(Z)-NCA]$_0$				unit ratio[b]	
run	DP[b]	M_w/M_n[b]	[MI]$_0$	time (day)	yield (%)	M($\times 10^{-3}$)[b]	*m*:*n*	M_w/M_n[c]
1	40	1.03	60	4	82	17.6	40:50	1.2
2	40	1.03	80	4	78	21.5	40:79	1.2

P*i*PrOx-PBLA[d]								
macroinitiator [MI]			[BLA-NCA]$_0$				unit ratio[e]	
run	DP[e]	M_w/M_n[c]	[MI]$_0$	time (day)	yield (%)	M_n ($\times 10^{-3}$)[e]	*m*:*n*	M_w/M_n[c]
3	40	1.03	60	3	90	16.2	40:57	1.2
4	40	1.03	80	3	98	20.9	40:80	1.1

[a] Solvent, DMF; [Lys(Z)-NCA]$_0$, 0.1 mmol/mL (run 1), 0.133 mmol/mL (run 2); temp, 37.5 °C. [b] Estimated by ^{1}H NMR in DMSO at 50 °C. [c] Estimated by GPC in DMF containing 10 mM LiCl at 40 °C. [d] Solvent, CH_2Cl_2; [BLA-NCA]$_0$, 0.2 mmol/mL (run 3), 0.267 mmol/mL (run 4); temp, 37.5 °C. [e] Estimated by ^{1}H NMR in DMSO at 50 °C (run 3) and $CDCl_3$ at 25 °C (run 4).

$M_n = 4500$, $M_w/M_n = 1.03$) (20 mg, 0.0044 mmol) in 1 mL of DMF and stirred at 37.5 °C for 4 days under a dry argon atmosphere. The polymerization was monitored by IR spectrometry. After confirming the disappearance of the *N*-carboxyanhydride (NCA) monomers, the mixture was concentrated under reduced pressure and added to 300 mL of *n*-hexane. The precipitate was dissolved in 1 mL of chloroform, followed by reprecipitation into 200 mL of diethyl ether to give P*i*PrOx-P(Lys(Z)) (yield: 82% (83 mg)). The composition of P*i*PrOx-P(Lys(Z)) was determined by GPC and ^{1}H NMR in DMSO-d_6.

Synthesis of Poly(2-isopropyl-2-oxazoline)-*b*-poly(L-lysine) Copolymer (P*i*PrOx-P(Lys)). P*i*PrOx-P(Lys(Z)) (83 mg, 5.4 × 10^{-6} mmol) (run 1 in Table 1) was dissolved in 5 mL of trifluoroacetic acid and stirred for 0.5 h. The solution was then added to 10 mL of a 30 wt % solution of HBr in AcOH, and the reaction mixture was stirred for 2 h at room temperature. Finally, the reaction mixture was precipitated in *n*-hexane, and the product was isolated by repeated precipitations. The product was then redissolved in distilled water and dialyzed against distilled water using a Spectrapor dialysis membrane with a 3500 M_r molecular weight cutoff value. P*i*PrOx-P(Lys) was obtained as a white powder after lyophilization (yield: 78% (65 mg)).

Synthesis of Poly(2-isopropyl-2-oxazoline)-*b*-poly(aspartic acid) Copolymer (P*i*PrOx-P(Asp)). β-Benzyl-L-aspartate NCA (BLA-NCA; 66 mg, 0.26 mmol) dissolved in 1 mL of dichloromethane was added to a solution of α-methyl-ω-amino-poly(2-isopropyl-2-oxazoline) (Me-P*i*PrOx-NH_2, M_n = 4500, M_w/M_n = 1.03) (20 mg, 0.0044 mmol) in 1 mL of dichloromethane and stirred at 37.5 °C for 3 days under a dry argon atmosphere. A procedure similar to that for P*i*PrOx-P(Lys(Z)) was also adapted for P*i*PrOx-PBLA (run 3 in Table 1). P*i*PrOx-P(Asp) was then prepared from P*i*PrOx-PBLA by the removal of the benzyl groups in 0.5 N NaOH at room temperature (reaction time 5 h). (yield: 95% (55 mg)).

Preparation of Polyion Complex Micelles. P*i*PrOx-P(Lys) and P*i*PrOx-P(Asp) were separately dissolved in a Tris-HCl buffered solution (10 mM, pH 7.4) with or without a varying NaCl concentration of 10, 100, and 150 mM, respectively. After filtration through a 0.4 μm filter (MILLEX-VV, Millipore), the polyion complex micelles were prepared by mixing these solutions in an equal unit ratio of L-lysine and aspartic acid residues in the block copolymers (total concentration: 1.0 mg/mL).

Dynamic Light Scattering (DLS) Measurements. All samples were stored overnight before the measurements and used without further purification. All measurements were performed at 20 °C. Details of the data analysis procedure have been described eleswhere.[4a,13]

Transmission Electron Microscopy (TEM). For the observation of the size and distribution of the micellar particles, a drop of the sample solution (concentration = 0.125 mg/mL) was placed onto a 400 mesh copper grid coated with a 0.5 wt % poly(vinyl formal) aqueous solution. About 2 min after deposition, the grid was touched with filter paper to remove the surface water, followed by air drying. Negative staining was performed using a droplet of a 1 wt % uranyl acetate solution. The samples were air dried before the measurement.

(12) (a) Daly, H. W.; Poche, D. *Tetrahedron Lett.* **1988**, *29*, 5859. (b) Fasman, G. D.; Idelson, M.; Blout, E. R. *J. Am. Chem. Soc.* **1961**, *83*, 709.

(13) (a) Xu, R.; Winnik, M. A.; Hallett, F. R.; Riess, G.; Croucher, M. D. *Macromolecules* **1991**, *24*, 87. (b) Harada, A.; Kataoka, K. *Macromolecules* **1998**, *31*, 288.

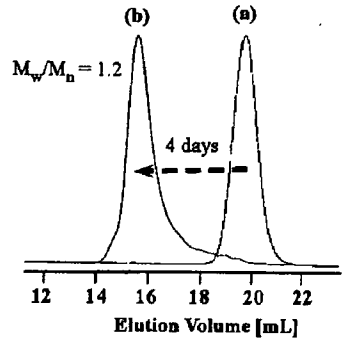

Figure 1. Gel permeation chromatograms of (a) Me-P*i*PrOx-NH_2 and (b) P*i*PrOx-P(Lys(Z)) (PEG standard; eluant, DMF (containing 10 mM LiCl); temperature, 40 °C; RI detection).

Turbidity Measurements Using the UV−Vis Spectrophotometer. The cloud points (T_{cp}) were determined by the spectrophotometric detection of the changes in the transmittance ($\lambda = 500$ nm) of the aqueous polymer solutions heated at a constant rate (0.5 °C min^{-1}). The samples were thermostated using a temperature-controlled circulating water bath. Cloud-point values of the polymer solutions were determined as the temperature corresponding to a 10% decrease in the optical transmittance.

Results and Discussion

Synthesis of Block Copolymers. In this study, ω-amino-terminated poly(2-isopropyl-2-oxazoline) (Me-P*i*PrOx-NH_2) (M_n = 4500, M_w/M_n = 1.03) was employed as a macroinitiator for the anionic ring-opening polymerization of NCA to form the block copolymers of P*i*PrOx and protected poly(amino acid) (P*i*PrOx-P(Lys(Z)) or P*i*PrOx-PBLA). The synthesized block copolymers were characterized by GPC and ^{1}H NMR as summarized in Table 1. Figure 1 shows the GPC profiles of the macroinitiator (Me-P*i*PrOx-NH_2) and the block copolymer (P*i*PrOx-P(Lys(Z))). After block copolymerization was carried out for 4 days, the peak shifted to a smaller elution volume because of an increase in the molecular weight. No peak of the macroinitiator remained, indicating the high efficiency of the block copolymerization. Figure 2 shows the ^{1}H NMR spectra of the block copolymer before (Figure 2a) and after (Figure 2b) the deprotection of the ϵ-benzyloxycarbonyl groups under the acidic conditions (30% HBr/AcOH) for run 1 in Table 1. Comparing the peak integral ratio of the methyl protons of P*i*PrOx ($(CH_3)_2$: δ 1.0) and the methylene protons of the ϵ-benzyloxycarbonyl group of P(Lys(Z)) ($CH_2C_6H_5$: δ 4.9), the DP of Lys(Z) was calculated to be 50. For P*i*PrOx-P(Lys) in Figure 2b, the peak integral ratio of the methyl protons of P*i*PrOx ($(CH_3)_2$: δ 1.0) and α-methine protons of P(Lys) (CO*CH*NH: δ 4.2) was measured in order to calculate the DP that was determined to be 52. It was confirmed from the similar DP values of lysine units for P*i*PrOx-P(Lys(Z)) and P*i*PrOx-P(Lys) that neither the loss of the lysine repeating units by backbone scission nor cleavage of the amide group to a secondary amino group in the side chain of the P*i*PrOx block occurred during the deprotection reaction. On the basis of these results, it was ascertained that the polymerization of Lys(Z)-NCA was successfully accomplished using the ω-amino-terminated P*i*PrOx macroinitiator: the polydispersity indices were about 1.2, and the experimental value of the degree of polymerization (DP) was close to the value predicted from the initial monomer/macroinitiator ratio (60/1). The P*i*PrOx-P(Lys) block ionomers (P*i*PrOx; M_n = 4500 g/mol) with different DP values of the P(Lys) segments, 52 and 82, are abbreviated 45C52 and 45C82, respectively.

In a similar fashion, the synthesis of P*i*PrOx-PBLA was performed as shown in Table 1 (runs 3 and 4). From the GPC

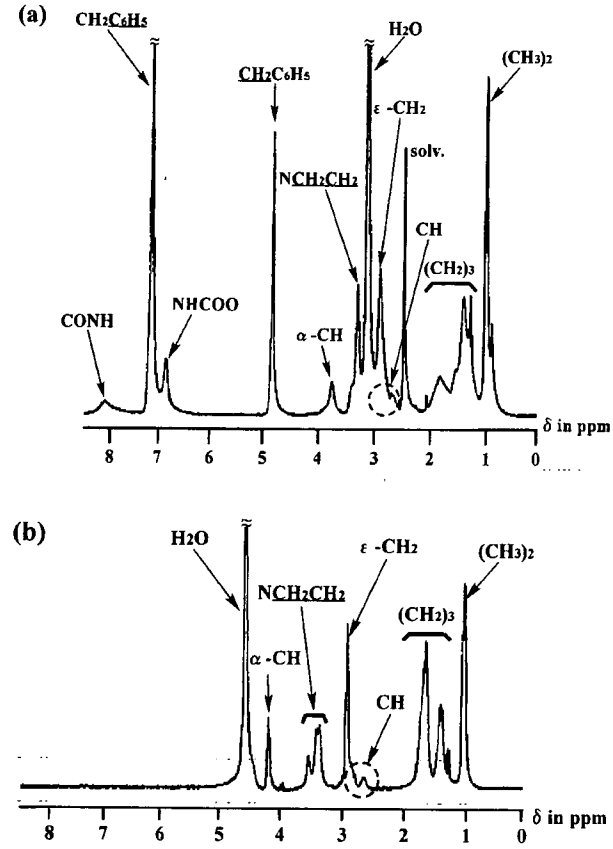

Figure 2. ^{1}H NMR spectra of (a) P*i*PrOx-P(Lys(Z)) in DMSO-d_6 at 50 °C and (b) P*i*PrOx-P(Lys) in D_2O at 20 °C.

of the obtained P*i*PrOx-PBLA (run 3 in Table 1, Figure S3 in Supporting Information), a unimodal peak was also observed in the reaction mixture after 3 days as in the case of P*i*PrOx-P(Lys-(Z)). To assign the composition of P*i*PrOx-PBLA, the ^{1}H NMR was measured in DMSO-d_6 (run 3) (Figure S4 in Supporting Information). From the peak integral ratio of the methyl protons of P*i*PrOx ($(CH_3)_2$: δ 1.0) to the benzyl protons of PBLA ($COOCH_2C_6H_5$: δ 7.2), the DP of BLA was determined to be 57. The ^{1}H NMR spectrum of P*i*PrOx-P(Asp) in D_2O, obtained after deprotection of the benzyl groups of P*i*PrOx-PBLA (run 3), is also shown in Figure S5 of Supporting Information. Although some of the peaks assigned to the methylene protons of the α,β linkages of P(Asp) (δ 2.7)[14] were superposed on a broad peak assigned to the methine proton of the isopropyl group of P*i*PrOx (δ 2.4−2.9), the DP (53) calculated from the integral ratio of the methyl protons of P*i*PrOx ($(CH_3)_2$: δ 1.0) to the methylene protons of the α,β linkages of P(Asp) (δ 2.7) was also in a good agreement with the result (DP = 57) for P*i*PrOx-PBLA. The P*i*PrOx-P(Asp) block ionomers (P*i*PrOx; M_n = 4500 g/mol) with different DP values of the P(Asp) segments, 53 and 76, are abbreviated 45A53 and 45A76, respectively.

Preparation of Polyion Complex Micelles. The PIC micelles were formed by mixing 1.0 mg/mL Tris-HCl solutions of P*i*PrOx-P(Lys) and P*i*PrOx-P(Asp) under stoichiometric conditions in which the unit ratio of the L-lysine in P*i*PrOx-P(Lys) and aspartate in P*i*PrOx-P(Asp) was unity. This procedure of PIC micelle formation by the simple mixing of a pair of oppositely charged

(14) (a) Yokoyama, M.; Miyauchi, M.; Yamada, N.; Okano, T.; Sakurai, Y.; Kataoka, K.; Inoue, S. *J. Controlled Release* **1990**, *11*, 269. (b) Yokoyama, M.; Inoue, S.; Kataoka, K.; Yui, N.; Okano, T.; Sakurai, Y. *Makromol. Chem.* **1989**, *190*, 2041.

Table 2. Size and Polydispersity Index Values of the PIC Micelles

samples	concentration (mg/mL)	D_T[a] (10^{-7}cm^2/s)	μ_2/Γ^2[a]	R_h[b] (nm)	diameter (nm) mean cumulative[a]	diameter (nm) z-weighted[c]	d_w/d_n[c]
45C52/45A53	1	1.306	0.078		36.2	37.0 ⊥ 8.4	1.16
	0.5	1.237	0.062	18.0	36.6	38.8 ± 7.7	1.15
	0.25	1.218	0.121		37.2	41.2 ± 13.1	1.21
	0.125	1.208	0.178		37.7	41.3 ⊥ 16.2	1.19
45C82/45A76	1	0.819	0.044		39.6	41.0 ± 8.7	1.11
	0.5	0.833	0.075	22.6	39.5	42.6 ± 12.0	1.17
	0.25	0.823	0.059		40.0	42.6 ⊥ 12.9	1.17
	0.125	0.822	0.044		40.1	41.8 ± 9.9	1.13

45C52/45A53 (1 mg/mL)	D_T[a] (10^{-7}cm^2/s)	μ_2/Γ^2[a]	diameter (nm) mean cumulative[a]	diameter (nm) z-weighted[c]	d_w/d_n[c]
10 mM NaCl	1.134	0.069	32.6	34.9 ± 9.1	1.15
100 mM NaCl	1.107	0.065	33.2	35.8 + 9.3	1.16
150 mM NaCl	1.048	0.094	36.6	37.6 ⊥ 8.8	1.13

[a] Obtained by cumulant analysis of dynamic light scattering (DLS). [b] Determined from the diffusion coefficient at infinite dilution (D_0) using the Stokes–Einstein equation. [c] Calculated by the histogram method. (d_w and d_n denote the weight- and number-average diameters, respectively.)

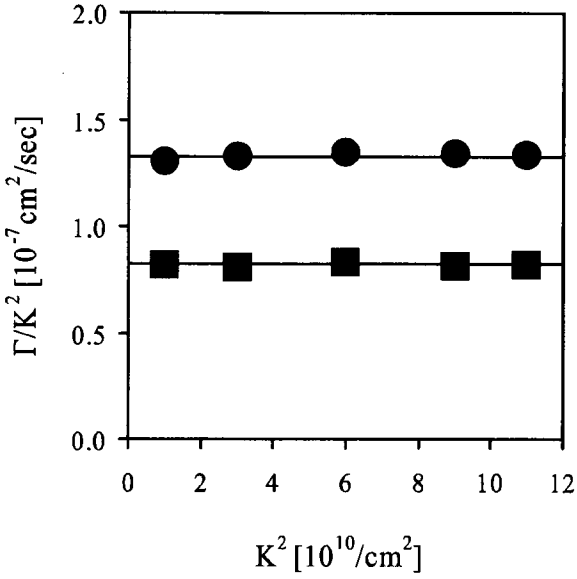

Figure 3. Relationship between the scaled average characteristic line width (Γ/K^2) and the magnitude of the scattering vector (K^2) for PIC micelles (45C52/45A53, ●; 45C82/45A76, ■; total concentration, 1.0 mg/mL; temperature, 20 °C; detection angles, 30, 60, 90, 120, and 150°; solvent, 10 mM Tris-HCl).

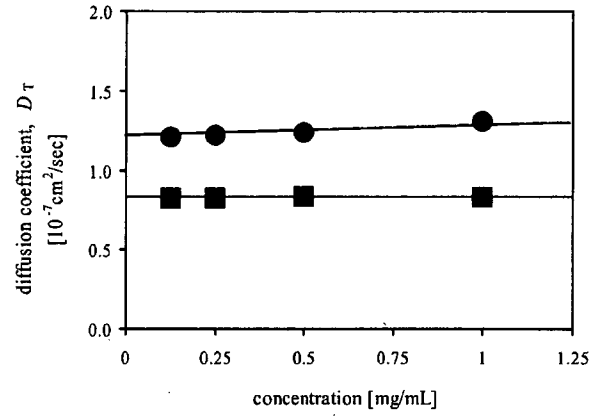

Figure 4. Plots of the translational diffusion coefficient (D_T) vs the total concentration of PIC micelles (45C52/45A53, ●; 45C82/45A76, ■; (temperature, 20 °C; detection angle, 90°; solvent, 10 mM Tris-HCl).

block ionomers had previously been established by our group for the PEG-P(Lys) and PEG-P(Asp) pair.[5a] The prepared solution was stored overnight in the refrigerator before DLS characterization.

Two pairs of PIC micelles were prepared by mixing the P*i*PrOx-based block ionomers with different charge lengths (Table 2): one comprising 45C52 where the unit number of L-lysine is 52 and 45A53 with the unit number of aspartate of 53 and the other comprising 45C82 where the unit number of L-lysine is 82 and 45A76 with the unit number of aspartate of 76. To investigate the shape as well as the size of the PIC micelles, angle-trace DLS measurements were carried out at 30, 60, 90, 120, and 150° detection angles at 20 °C. The sufficiently low temperature condition (20 °C) had to be adapted for all of the sample measurements, excluding the unexpected change in the shape or size of the PIC micelles, possibly derived from the collapse of the P*i*PrOx segments around the phase-transition temperature. Figure 3 shows the relationship between the scaled average of the scattering characteristic line width (Γ/K^2) and the magnitude of the scattering vector (K^2) at a concentration of 1 mg/mL. The Γ/K^2 values of the PIC micelles formed between P*i*PrOx-P(Lys) and P*i*PrOx-P(Asp) were independent of the detection angle in all cases. These results agreed with the fact that the Γ/K^2 values should be independent of the detection angle in the case of spherical particles. Because the angular dependence of Γ/K^2 was almost negligible, the following DLS measurements were performed at a 90° detection angle.

Figure 4 shows the concentration dependence of the diffusion coefficient (D_T). The PIC micelles were prepared by mixing the solutions of P*i*PrOx-P(Lys) and P*i*PrOx-P(Asp) (45C52/45A53 and 45C82/45A76 in Table 2) with diluting concentrations from 1 to 0.125 mg/mL under an electrostatically neutralized condition (1:1 unit ratio of L-lysine and aspartate residues). It is obvious that the diffusion coefficients were almost independent of the concentrations of both 45C52/45A53 and 45C82/45A76, indicating that the change in the total concentration induces no formation of secondary aggregates. It is likely that the P*i*PrOx shell layer may prevent the clustering of the micelles due to a steric repulsion mechanism, which is consistent with the formation of a core–shell structure. The diffusion coefficient at infinite dilution D_0 was then determined to be 1.187×10^{-7} cm^2/s (from 45C52/45A53 in Table 2) and 0.822×10^{-7} cm^2/s (from 45C82/45A76 in Table 2), respectively, for the 45C52/45A53 and 45C82/45A76

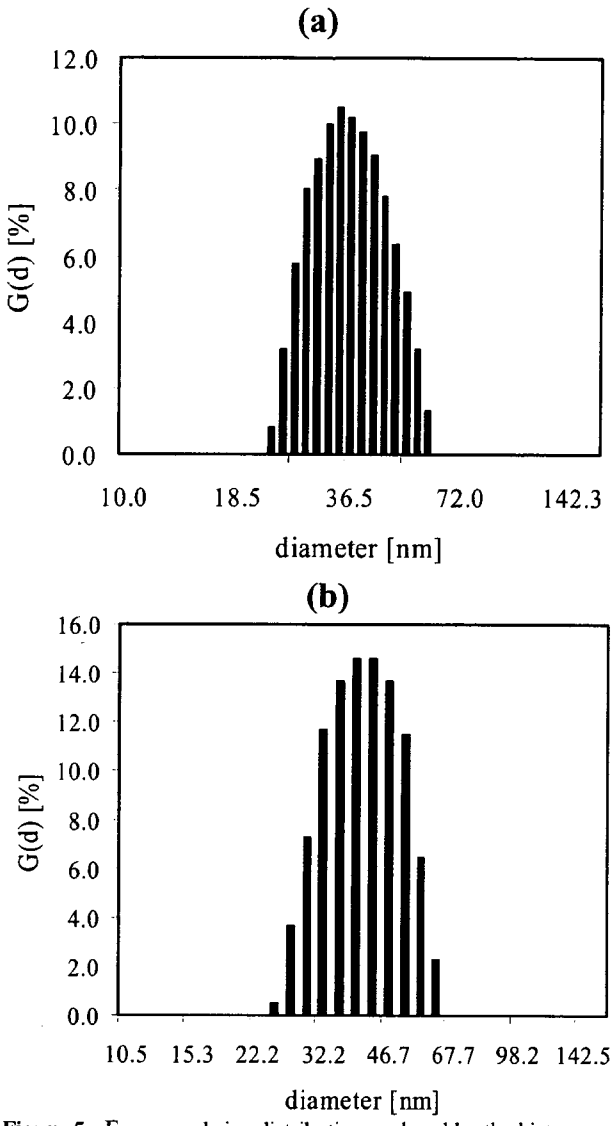

Figure 5. Γ-averaged size distribution analyzed by the histogram method for PIC micelles: (a) 45C52/45A53 and (b) 45C82/45A76 (total concentration, 1.0 mg/mL; temperature, 20 °C; detection angle, 90°; solvent, 10 mM Tris-HCl).

systems. From the obtained D_0 value, values of the hydrodynamic radius (R_h) were calculated to be 18.0 and 22.6 nm using the Stokes–Einstein equation. Obviously, the R_h values slightly increased with an increase in the length of the charged segments. The polydispersity indices (μ_2/Γ^2) (Table 2) were small enough to consider that the micelles have a narrow size distribution. This narrow size distribution is in good agreement with the result of the independence of the Γ/K^2 value versus the detection angle, as shown in Figure 3.

Figure 5 shows the Γ-averaged size distribution of the polyion complex micelles (1 mg/mL) obtained from the histogram analysis of the DLS data at 20 °C. It was confirmed from the size distribution profiles that the micelles prepared were unimodal with average diameters of 37.0 ± 8.4 and 41.0 ± 8.7 nm, respectively (Figure 5a and b for the 45C52/45A53 and 45C82/45A76 systems). These were in good agreement with the mean cumulative diameters (36.2 and 39.6 nm) and R_h values (18.0 and 22.6 nm) calculated from the cumulant analysis. All of the data including the polydispersity index (d_w/d_n) values obtained from this histogram method are also summarized in Table 2.

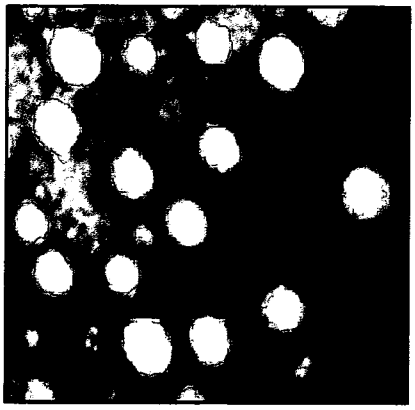

Figure 6. TEM image of PIC micelles formed from 45C52 and 45A53 in distilled water at room temperature (concentration, 0.125 mg/mL; negative staining by a 1 wt % uranyl acetate solution).

Furthermore, it was confirmed that monodisperse spherical particles with an ~40 nm diameter were clearly observed in the TEM image of the PIC micelles from 45C52/45A53 prepared in distilled water (Figure 6).

The electrophoretic mobility of the PIC micelle (45C52/45A53) was also determined to be −0.04745 ± 0.0105 μm cm/Vs on the basis of laser-Doppler electrophoresis. The average ζ-potential was then calculated from this value using the Smoluchowski equation.[5a] The calculated average ζ-potential of the PIC micelles had an extremely small absolute value (−0.6690 ± 0.148 mV), indicating the shielding of the PIC core by the electrically neutral shell of the P*i*PrOx segments.

On the basis of the results of the DLS, TEM, and ζ-potential described above, it is reasonable to conclude that the micelles having the PIC core were surrounded by P*i*PrOx as the shell layer and were stably dispersed with a narrow, unimodal distribution in an aqueous entity at 20 °C. It is known that the stability of the polyion complex is strongly affected by the ionic strength of the medium (i.e., destabilized with an increase in the ionic strength due to electrostatic shielding[15]). The effect of the ionic strength on the stability of the PIC micelles was estimated by measuring the size of the PIC micelle solutions (1 mg/mL) under several NaCl concentrations. The diffusion coefficients (D_T) remained constant almost up to the 150 mM NaCl concentration value, viz., near physiological conditions, meaning that the stability of the PIC micelles is sufficient under the measured ionic strengths (Table 2 and Figure 7a–c).

Determination of the Cloud Points (T_{cp}). As the first step in our study of the thermoresponsive behavior of the P*i*PrOx-based PIC micelles, we examined in detail the cloud-point (T_{cp}) values of the P*i*PrOx oligomer solutions. It was necessary to select two parameters, such as the oligomer and NaCl concentrations, when considering the future application of the PIC micelles under physiological conditions. In addition, ω-acrylate-terminated P*i*PrOx (Me-P*i*PrOx-acrylate) was prepared by end capping the ω-hydroxyl group of Me-P*i*PrOx-OH in order to explore the effects of the terminal end groups on T_{cp}, which are presumably pronounced for the oligomer solutions.

The open (in the absence of NaCl) and closed (in the presence of 150 mM NaCl) symbols in Figures 8a and b show the turbidity changes in the aqueous solutions of Me-P*i*PrOx-OH (M_n = 4500, M_w/M_n = 1.03) (square symbols) and Me-P*i*PrOx-acrylate (M_n = 4500, M_w/M_n = 1.03) (circle symbols) bearing the same chain length as that used in the synthesis of the block ionomers under

(15) (a) Abe, K.; Ohno, H.; Tsuchida, E. *Makromol. Chem.* **1977**, *178*, 2285. (b) Tsuchida, E.; Osada, Y.; Ohno, H. *J. Macromol. Sci. Phys.* **1980**, *B17*, 683.